ONLINE SUPPLEMENTAL DOCUMENT

Vinculin Phosphorylation Impairs Vascular Endothelial Junctions Promoting Atherosclerosis Associated with Disturbed Flow

by

Yu-Tsung Shih, Ph.D.[1], Shu-Yi Wei, Ph.D.[1,δ], Jin-Hua Chen, Ph.D.[2,δ], Wei-Li Wang, Ph.D.[1], Hsin-Yi Wu, Ph.D.[3], Mei-Cun Wang, M.S.[1], Chia-Yu Lin, B.S.[1], Pei-Lin Lee, B.S.[1], Chih-Yuan Lin, M.D., Ph.D.[4], Hung-Che Chiang, M.D., Ph.D.[5], Yu-Ju Chen, Ph.D.[6], Shu Chien, M.D., Ph.D.[7], and Jeng-Jiann Chiu, Ph.D.[1,8,9,*]

[1] Institute of Cellular and System Medicine, National Health Research Institutes, Miaoli 35053, Taiwan
[2] Graduate Institute of Data Science, College of Management; Health Data Analytics and Statistics Center, Office of Data Science; Biostatistics Center, Department of Medical Research, Wan Fang Hospital, Taipei Medical University, Taipei 11031, Taiwan.
[3] Instrumentation Center, National Taiwan University, Taipei, 10617, Taiwan
[4] Division of Cardiovascular Surgery, Tri-Service General Hospital, Taipei 114, Taiwan
[5] Department of Pharmacy, School of Pharmacy, China Medical University, Taichung, Taiwan
[6] Institute of Chemistry, Academic Sinica, Taipei 11529, Taiwan
[7] Departments of Bioengineering and Medicine, and Institute of Engineering in Medicine, University of California, San Diego, La Jolla, CA 92093, USA
[8] School of Medical Laboratory Science and Biotechnology; Ph.D. Program in Medical Biotechnology, College of Medical Science and Technology; Taipei Heart Institute, Taipei Medical University, Taipei 11031, Taiwan
[9] Institute of Biomedical Engineering, National Tsing Hua University, Hsinchu 30071, Taiwan

ONLINE SUPPLEMENTAL METHODS

Materials. Mouse monoclonal antibodies (mAbs) against human VE-cadherin (sc-9989) and platelet endothelial cell adhesion molecule-1 (PECAM1) (sc-18916) were purchased from Santa Cruz Biotechnology (Dallas, TX, USA). A mouse mAb against CD68 (ab125212) and rabbit polyclonal antibodies (pAbs) against smooth muscle-22α (SM22α) (ab155272), RFP

(ab124754), and smooth muscle α-actin (αSMA) (ab32575) were purchased from Abcam (Trumpington, CB, UK). Alexa Fluor 488 conjugation kit (ab236553, Abcam) for pre-labeling the VCL^{S721p} antibody was purchased from Abcam. Mouse mAbs against α-catenin (13-9700), β-catenin (13-8400), DDK-tag (TA50011-100), isolectin B4 (IB4) (I21414), and siRNAs against GRK2 (VHS50690), β_1 integrin (HSS105561), and β_3 integrin (HSS105567) were purchased from Invitrogen (Thermo Fisher Scientific). Rabbit pAbs against αv integrin (#4711), α_5 integrin (#4705), β_1 integrin (#9699), β_3 integrin (#13166), CD9 (#13403), endothelial nitric oxide synthase (eNOS) (#9572) and $eNOS^{S1077p}$ (#9571) were purchased from Cell Signaling (Danvers, MA, USA). Rabbit pAbs against vinculin (VCL) (GTX113294), G protein-coupled receptor kinase 2 (GRK2) (GTX101682), transferrin (GTX21223), Tek (GTX107505), Caveolin-2 (Cav2) (GTX108294), VCL^{Y1065p} (GTX54518), VCL^{Y100p} (GTX54517), and VCL^{Y822p} (GTX54519) were purchased from GeneTex (Irvine, CA, USA). The generation of GRK2 pre-labeled with Alexa Fluor-594 was supported by GeneTex (HsinChu, Taiwan). A rabbit pAb against $GRK2^{S29p}$ (A0486) was purchased from Assay Biotech (Fremont, CA, USA). Rabbit anti-$Cav2^{S23p}$ antibody (A50786) was purchased from Antibodies (Station Road, Cambridge, UK). Mouse Ab against human CD144-conjugated PE (348505), isotype control IgG (401407), and rabbit polyclonal isotype control antibody (910805) were purchased from Biolegend (San Diego, CA, USA). Mouse anti-von Willebrand Factor (vWF; AB7356), anti-μ-calpain (MAB3083), anti-HUTS-4 (MAB2079Z), and anti-LIBS-2 (MABT27) antibodies were purchased from Millipore (Temecula, CA, USA). A small molecule GRK2 inhibitor (CAS24269-96-3) was purchased from Calbiochem (San Diego, CA, USA). Atorvastatin calcium (PHR1422) was purchased for the animal experiments from Sigma-Aldrich (St. Louis, MO, USA). Atorvastatin calcium (S2077) for *in vitro* studies was purchased from Selleckchem (Houston, TX, USA). The VCL (RC219299) and GRK2 (RC210327) plasmids were purchased from OriGene (Rockville, MD,

USA). Fluorescence-conjugated donkey anti-mouse (A21202) and anti-rabbit (A21207) IgG secondary antibodies were purchased from Life Technologies (Carlsbad, CA, USA). ExoCET Exosome Quantitation Assay (ExoCET96A-1), Exo-Flow Purification Kit (EF32A-CD9), and Exo-Quick (EXOQ5A-1) were purchased from System Biosciences (Mountain View, CA, USA). All other chemicals of reagent grade were obtained from Sigma-Aldrich unless noted otherwise.

***Ex Vivo* Porcine Endothelial Cell (EC) Collection and Characterization.** Porcine aortas were obtained from PigModel Animal Technology Co., Ltd. (Miaoli, Taiwan). After the experimental pig (Landrace X Yorkshire males, 230–250 pounds, 6–7 months of age) was sacrificed, the heart and aorta arch were rapidly removed from the thoracic cavity and placed in cold saline containing a phosphatase inhibitor cocktail (PhosSTOP and cOmplete tablets from Roche), a mixture of several inhibitors containing serine-threonine phosphatase inhibitors and tyrosine phosphatase inhibitors, which protect valuable proteins from dephosphorylation. ECs were freshly harvested from the ascending aorta, aortic arch, and descending thoracic aorta of six to eight adult pig aortas. ECs were gently scraped using a cryogenic procedure from the areas (1 cm^2 each) located at the inner and outer curvatures of the aortic arch and the dorsal descending thoracic aorta. Each cell sample was transferred to 100 μL of lysis buffer containing phosphatase inhibitors guanidine isothiocyanate and β-mercaptoethanol (0.143 M) (Qiagen, Germantown, MD, USA) and frozen on dry ice. To assess the purity of cell populations, fresh endothelial isolations from the aortic regions were measured by indirect immunofluorescence using flow cytometry, immunoblotting, and immunocytochemistry staining. For flow cytometry analysis, cells were fixed with 2% paraformaldehyde at 4°C for 10 min and stained with two fluorescence- or biotin-conjugated antibodies (0.5 μg/mL) against VE-cadherin and SM22α. The latter was detected with a

fluorescence-labeled secondary antibody. Fluorescence-labeled cells (~10^4 cells/sample) were analyzed with a fluorescence-activated cell sorter (FACSCalibur, Becton-Dickinson, Franklin Lakes, NJ). Isotype-matched antibodies served as controls in every experiment. The experimental protocol was approved by the Institutional Animal Care and Use Committee (IACUC) of the National Health Research Institutes in Taiwan (NHRI-IACUC-103125-A). The detailed procedures of FACS were described previously [1].

Phosphoproteomics Analysis. The phosphoproteomics data were analyzed with an LTQ-Orbitrap Velos mass spectrometer at the Academia Sinica Common Mass Spectrometry Facilities in Taiwan, as previously described.[2,3] Briefly, protein samples from porcine aortic endothelium (~1 mg total protein, each sample from six independent pigs) were subjected to gel-assisted digestion for extraction of tryptic peptides, an IMAC procedure for phosphopeptide enrichment, triplicate LC-MS/MS analysis, and RAW2MSM software for phosphopeptide/phosphoprotein sequence searches, and quantitative analysis using IDEAL-Q software. Targeted protein screening manually identified proteins of interest. The implications of protein phosphorylation were assessed by cross-referencing the phosphorylation of proteins with libraries of common signaling pathways listed in GeneCards (www.genecards.org) for a given protein. The phosphorylation function was determined using the phosphorylation site database PhosphoSitePlus® (www.phosphosite.org).

Cell Culture. Human aortic ECs were purchased from Cell Applications (San Diego, CA, USA) and cultured in EC growth medium (#213-500, Cell Applications) supplemented with 10% FBS (Gibco, Waltham, MA, USA) and 1% penicillin/streptomycin (Gibco). ECs (1-2×10^5 cells/cm^2) were grown in Petri dishes for 3 d and then seeded onto glass slides (75×38 mm, Corning, NY, USA) pre-coated with fibronectin. Cells between passages 3 and 5

were used in all experiments.

Flow Apparatus. Cultured ECs were subjected to shear stress in a parallel-plate flow chamber, as previously described.[4] Briefly, the flow channel in the chamber was created by a 2.5 cm-wide × 5.0 cm-long × 0.025 cm-high silicon gasket. The chamber containing the cell-seeded glass slide fastened with the gasket was connected to a perfusion loop system, kept in a temperature-controlled enclosure, and maintained at pH 7.4 by continuous gassing with a humidified mixture of 5% CO_2 in the air. The oscillatory shear stress (OS) was composed of a low level of mean flow with shear stress at 0.5 dynes/cm^2 supplied by a hydrostatic flow system to provide essential nutrient and oxygen delivery and the superimposition of a sinusoidal oscillation using a piston pump with a frequency of 1 Hz and a peak-to-peak amplitude of ±4 dynes/cm^2. In parallel experiments, ECs were kept under static condition or exposed to pulsatile shear stress (PS) at 12±4 dynes/cm^2. In some experiments, ECs were incubated with a GRK2-specific inhibitor (30 μM) or atorvastatin (1 μM) for 24 h in the flow apparatus.

Western Blot Analysis. Cells were lysed with a buffer containing 1% Nonidet P-40, 0.5% sodium deoxycholate, 0.1% SDS, and a protease inhibitor mixture (PMSF, aprotinin, and sodium orthovanadate). The total cell lysate (100 μg of protein) was separated by SDS/PAGE (10% running, 4% stacking) and analyzed using the designated antibodies, as previously described.[4] Proteins extracted from mouse organs/tissues were homogenized using an electric homogenizer. The lysis buffer was added during homogenization. In some experiments, cells were treated with recombinant human epidermal growth factor (EGF; 236-EG, R&D, Minneapolis, MN, USA) to activate GRK2.

Animal Model of Aortic Stenosis. We induced stenosis of the male rat abdominal aorta using a U-shaped titanium clip, as previously described.[5] Briefly, after anesthetization with isoflurane, the rat abdominal aorta (segment between the renal artery and the iliac artery) was exposed, and the clip was held with a pair of forceps and placed around the isolated segment (~1 cm proximal from the iliac arterial bifurcation) to partially constrict the abdominal aorta, leading to localized stenosis. Two d after surgery, the flow pattern and shear stress in different locations of the rat abdominal aorta were measured by Doppler ultrasound to confirm aortic stenosis. The rats were euthanized 7 d after surgery, and the aorta was perfusion-fixed with 4% paraformaldehyde at 120 mm Hg. The fixed aorta was embedded in paraffin blocks for immunohistochemical studies. All rats were provided with a regular diet. Animal experiments were performed following National Institutes of Health guidelines and with the approval of the Animal Research Committee of the National Health Research Institutes (NHRI-IACUC-106129-M).

Immunohistochemical Staining. Samples were snap-frozen in optical coherence tomography (OCT)-embedded compound (16-004004, Lab-Tek, Van Nuys, CA, USA) and stored at −80°C until use. The detailed procedures of immunohistochemical staining were previously described.[1] Briefly, serial sections (5 μm thick) of mouse aorta or human atheromas were placed on poly-L-lysine-coated slides and blocked for 1 h with tris-buffered saline (TBS) containing 5 mg/mL serum albumin. The specimens were incubated with antibodies against rabbit TeK, αSMA, RFP, VCL^{S721p}, $GRK2^{S29p}$ or mouse vWF, CD68, VE-cadherin, VCL, GRK2 (1:100-1:200) or isolectin B4-conjugated Alexa Fluor 647 (1:1000) overnight at 4°C, followed by Alexa Fluor 488/594/647-conjugated secondary antibodies for 1 h at room temperature. In some experiments, specimens were co-immunostained for two designated molecules. In the co-localization experiments, the rabbit VCL^{S721p} antibody was

pre-labeled with fluorescence dye by Alexa Fluor-488 conjugation kit. Species-matched isotype IgG was used instead of the primary antibody as a negative control. All photomicrographs were taken with an epifluorescence microscope (Axioplan 2; Zeiss, Gottingen, Germany) or a confocal microscope (TCS Sp5II; Leica). Invading macrophages were quantified as the number of CD68-positive cells per mm^2 in the interior of the neointimal area. Fluorescence intensities of VCL^{S721p} and $GRK2^{S29p}$ in the VE-cadherin-labeled endothelial layer were examined by confocal microscopy with Leica Microsystem LAS AF software. The average fluorescence intensity value in the endothelial layer and the number of invaded macrophages were calculated for all images from each mouse and human specimen.

Generation of Anti-VCL^{S721p} Antibody. A specific polyclonal antibody against VCL^{S721p} was prepared using the service provided by AbKing Biotechnology Co., Ltd (Taipei, Taiwan). Pathogen-free male rabbits (New Zealand white rabbits) were immunized with peptide CAIDTK(pS)LLDA (0.5 mg) conjugated to OVA (ovalbumin) followed by repeated boosts (0.25 mg per 14 d, three times). Serum was collected 60 d after the initial immunization and screened by enzyme-linked immunosorbent assay (ELISA). Serum displaying a robust immune response was used for double affinity purification. Serum was passed over a column containing the peptide CAIDTKSLLDA, and the flow-through was affinity-purified on a column containing CAIDTK (pS)LLDA phosphopeptide. In the co-localization experiments, the rabbit VCL^{S721p} antibody was pre-labeled with fluorescence dye by the Alexa Fluor-488 conjugation kit.

Phosphorylated Site Mutagenesis. The serine-721 substitution in the VCL plasmids (#RC219299, OriGene and #46276, Addgene) was created using a site-directed mutagenesis

approach with QuikChange Lightning multi-site-directed mutagenesis kits (#210514, Agilent, Santa Clara, CA, USA), according to the manufacturer's instructions. The detailed procedures of phosphorylated site mutagenesis were previously described.[3] The mutation of serine-721 to alanine (A) in the VCL plasmid was generated as non-phosphorylatable VCL^{S721A}, and the mutation to glutamine acid (E) was generated as phosphomimetic VCL^{S721E}. The primer sequences used for mutagenesis are available upon reasonable request. All vector sequences were verified by DNA sequencing.

siRNA and DNA Plasmid Transfection. For siRNA transfection, ECs at 70–80% confluence were transfected with the designed RNA at various concentrations (5–30 nM) for 24 or 48 h using the Invivofectamine™ Kit (#IVF3005, Invitrogen) before shear stress experiments. A non-targeting siRNA control served as a negative control in every experiment. After transfection, the cells were kept as static controls or subjected to OS or PS. In some experiments, ECs were transfected with VCL plasmid, mutated VCL plasmids, empty plasmid pET-15b using X-tremeGene HP DNA Transfection Reagent (#06366236001, Roche), or TurboFect Transfection Reagent (R0531, ThermoFisher), as previously described.[1]

Fluorescence Resonance Energy Transfer (FRET). The VCL FRET tail probe was a gift from Susan Craig (#46276, Addgene plasmid) and was modified from serine-721 to alanine or glutamine using QuickChange Lightning multi-site-directed mutagenesis kits. All fluorescence imaging of VCL FRET tail probes with/without specific site mutations (S721A or S721E) and photobleaching experiments were performed using a confocal microscope (TCS SP5II; Leica). Glass slides with fluorescent-labeled live cells were placed on 37°C plate heater during imaging. Calculations were performed using custom-written programs for FRET acceptor photobleaching in Leica LAS AF Systems. VCL FRET and donor channel

images were background-subtracted. We corrected for photobleaching by taking the overall fluorescence intensity of each image (excluding background) and that value to normalize each image to its corresponding image at the first time point. Mean values of FRET efficiency imaging within the bleached region were then generated, and the intensity was calculated by the Leica LAS AF program. All images were acquired at 1024 x 1024 pixels, with a pixel size of 0.5 μm. Fluorescence images were optimized for contrast and brightness using Image J 1.52a for demonstration purposes.

Immunoprecipitation. The detailed procedures of immunoprecipitation were previously described.[4] Briefly, ECs were lysed with a buffer containing 25 mM Hepes pH 7.4, 1% Triton X-100, 1% deoxycholate, 0.1% SDS, 0.125 M NaCl, 5 mM EDTA, 50 mM NaF, 1 mM Na3VO4, 1 mM PMSF, 10 mg/mL leupeptin, and 2 mM β-glycerophosphate. The same amount of protein from each sample was incubated with antibodies for 2 h at 4°C, followed by incubation with protein A/G plus agarose for 1 h. The agarose-bound immunoprecipitates were collected by centrifugation and incubated with a boiling sample buffer containing 62 mM Tris·HCl pH 6.7, 1.25% (wt/vol) SDS, 10% (vol/vol) glycerol, 3.75% (vol/vol) mercaptoethanol, and 0.05% (wt/vol) bromophenol blue and then subjected to SDS/PAGE and Western blot analysis.

***In Situ* Proximal Ligation Assay (PLA).** *In situ* PLA was performed with a Duolink® *In Situ* Red Starter Kit and followed the manufacturer's protocols (Duo92101, Olink Bioscience, Uppsala, Sweden), as previously described.[4] Briefly, after exposure to OS or PS for 24 h, cells were fixed with 4% (wt/vol) paraformaldehyde for 20 min, permeabilized with 0.1% Triton X-100 in PBS containing 1% BSA for 20 min, incubated with rabbit anti-VCL or anti-VCL^{S721p} antibody and incubated with mouse anti-α-catenin or β-catenin antibody at

37°C for 1 h. After three washes in PBS, the cells were labeled with PLUS oligonucleotide-conjugated anti-mouse antibody and MINUS oligonucleotide-conjugated anti-rabbit antibody at 37°C for 1 h. After adding template oligonucleotide, annealing, and ligation, the circularized template was amplified via polymerase; the amplified sequence was detected by hybridization with a Texas Red-labeled probe. Secondary antibodies were used as controls to distinguish the target staining from the background. The cells were examined and photographed by fluorescence confocal microscopy (TCS SP5II; Leica).

***In Vitro* Endothelial Permeability Assay.** Permeability was assessed by passing FITC-conjugated dextran (~70 kDa) through the EC monolayer, as previously described.[6] Briefly, 1×10^5 ECs transfected with different plasmids were seeded on the apical side of a 24-well transwell fibronectin-coated insert with 0.4-μm pores (Thermo Fisher Scientific, Waltham, MA, USA), allowed to grow overnight to full confluence for the formation of a monolayer, and growth-arrested for 6 h. The blank in the endothelial permeability assay represented "no ECs" on the upper chamber of the transwell system. FITC-conjugated dextran (FD70S, Sigma-Aldrich) was added (100 μg/ml) to the basal chamber. After 0.5 h or 1 h of incubation, 100 μl of the medium from each chamber was collected, and the fluorescence intensity was measured using a spectrofluorometer (excitation, 490 nm; emission, 520 nm). A standard curve with FITC-dextran (0–2 mg/ml) was also prepared in each experiment and simultaneously read by a microplate reader (Infinite® M200, Tecan Trading AG, Switzerland). All experiments were performed in triplicate, and the results are expressed as permeability relative to control cells.

Generation of EC-specific bacterial artificial chromosome (BAC) transgenic (Tg) *Vcl*^{S721A}*ApoE*$^{-/-}$ mice. The generation of EC-specific Tg mouse lines was supported by the

National Laboratory Animal Center, Taiwan. The experimental protocol was approved by the IACUC of Taiwan's National Health Research Institutes (NHRI-IACUC-106129-M and NHRI-IACUC-109015-A). To generate endothelium-specific Tg mice, a BAC plasmid containing the EC-specific mouse Tek promoter/enhancer was ligated with the coding mutation sequence of mouse VCL^{S721A} cDNA and the reporter gene RFP. This BAC clone was sequenced as a mTek-RFP-IRES-Flag-Vcl^{S721A}-pA-expressing cassette and named Tek-Vcl^{S721A}, as shown in *Figure S9A*. The RFP-encoding sequence was introduced to the cassette to allow Vcl^{S721A} protein detection. EC-specific Tg mouse lines ($_{EC}Vcl^{S721A}$ mice) were established by pronuclear microinjection of linearized Tek-Vcl^{S721A} plasmid into fertilized C57BL/6 eggs. $_{EC}VCL^{S721A}$ Tg mice overexpressing VCL^{S721A} in ECs under the Tek promoter/enhancer control were crossed with $ApoE^{-/-}$ mice (Jackson Laboratories, USA) to generate matched litters of heterogeneous $_{EC}Vcl^{S721A}ApoE^{-/-}$ and inbred control $ApoE^{-/-}$ mice. Furthermore, homogeneous $_{EC}Vcl^{S721A}ApoE^{-/-}$ inbred mice were obtained by crossbreeding heterogeneous $_{EC}Vcl^{S721A}ApoE^{-/-}$ mice and confirmed by crossing with $ApoE^{-/-}$ mice. Positive Tg mice were identified by standard PCR analysis of genomic DNA (*Figure S9B*), and protein expression was further confirmed by Western blotting (*Figure S9C*), and *en-face* immunohistochemical staining (*Figure S9D*). The PCR primer nucleotide sequences (5' →3') were: (1) mutant ApoE genotyping: common forward primer GCCTAGCCGAGGGAGAGCCG and mutant reverse primer GCCGCCCCGACTGCATCT; (2) wild-type ApoE: common forward primer GCCTAGCCGAGGGAGAGCCG and wild-type reverse primer TGTGACTTGGGAGCTCTGCAGC; and (3) RFP: forward primer TGGCTACCAGCTTCATGTACGG and reverse primer TTGCTAGGGAGGTCGCAGTATC. $_{EC}Vcl^{S721A}ApoE^{-/-}$ mice were crossed for at least five generations for animal experiments. Male mice were chosen in this study to avoid the potential impact of periodic sex hormone fluctuations on atherosclerosis. Male $_{EC}Vcl^{S721A}ApoE^{-/-}$ and inbred control $ApoE^{-/-}$ littermates

were fed normal chow or high-cholesterol diet (HCD, 4.5 kcal/g, 20% fat and 1.25% cholesterol; D12108C, Research Diet Inc, New Brunswick, NJ, USA) for 6–18 weeks beginning at 6 weeks of age. We detected the mice's aortic vascular tone and heart sinus rhythm at the end of the experiments. Organs, including heart, lung, live, thigh muscle, spleen, and kidney, were also collected for analyzing endogenous VCL and VCL^{S721p} levels. Blood was collected from these mice to determine the plasma lipid profiles and for serum chemistry assays (*Table S2*) using Fuji Dri-Chem slides (Fujifilm Dri-Chem 4000, Tokyo, Japan) following the manufacturer's protocol. Researchers were blinded to the genotypes of the animals until analysis completion.

***ApoE*$^{-/-}$ Mouse Experiments**. ApoE-knockout (*ApoE*$^{-/-}$) mice on a C57BL/6 background were purchased from Jackson Laboratory (Bar Harbor, ME, USA). The experimental protocol was approved by the IACUC of Taiwan's National Health Research Institutes (NHRI-IACUC-106129-M and NHRI-IACUC-109015-A). Six-week-old male *ApoE*$^{-/-}$ mice received vehicle controls (saline) or GRK2 inhibitor (10 mg/kg *IV*, every 3 d) with an HCD for 6–18 weeks. These mouse groups received an intravenous injection of saline or GRK2 inhibitor three times per week. Blood was collected from these mice to determine the plasma lipid profiles and serum chemistry assays (*Table S3*). For *in vivo* transfection, the VCL^{S721A} plasmid was injected slowly into the tail veins of mice at a dosing volume of 8 ml/kg TurboFect *in vivo* transfection reagent (R0541, Thermo Fisher) per mouse in two doses of 2 mg DNA/kg per week for histological examinations. The transgene delivery was evaluated by *en-face* and immunohistochemical staining with tag protein/peptide DDK in the isolectin B4-positive endothelium layer of the mouse aorta. In the atorvastatin experiments, 6-week-old male mice were randomly divided into control and atorvastatin groups. Atorvastatin was dissolved in isosmotic saline and infused via a stomach tube at a dose of 10

mg/kg/d after surgery for 6–18 weeks. Controls were infused with an equal volume of isosmotic saline. The mice had free access to water and food during the entire period. Photomicrography and image analysis were performed by a team member who was unaware of the source of reagents to avoid bias. Researchers were blinded to the groups of animals until analysis completion.

***En-face* Preparation and Staining.** The procedures were described in detail previously.[3,4] Briefly, the mice were euthanized with an overdose of CO_2 and transcardially perfused with 50 mL of saline, followed by 100 mL of 10% (vol/vol) neutral-buffered zinc-formalin (#57052F, Thermo Fisher Scientific). After perfusion, the affected aortas were harvested and postfixed in this fixative solution for 1 h and then subjected to *en-face* immunostaining. Tissues were washed with TBS buffer, and the adventitia was carefully removed. The aortas were longitudinally dissected with micro dissecting scissors and pinned flat on a black wax dissection pan. The luminal surface of the aorta was immediately blocked with 4% (vol/vol) FBS for 1 h, followed by incubation with the designated primary antibodies (1:50) at 4°C overnight. Alexa Fluor 594-conjugated anti-rabbit IgG (1:500; Invitrogen) and Alexa Fluor 488-conjugated anti-mouse IgG (1:500; Invitrogen) were used as secondary antibodies. Samples were counterstained with DAPI to show cell nuclei, rinsed three times in TBS, mounted with glycerol/PBS (1:1), and photographed with a confocal microscope (TCS SP5II; Leica). Secondary antibodies were used as controls to distinguish the target staining from the background. To determine the gap area in the endothelium, images from all channels were overlaid to visualize all stained components. Monolayer disruption was quantified by determining the area of each 63X image occupied by intercellular space. Briefly, different thresholds were manually investigated for cells representing the range of brightness throughout the sample images to determine the threshold value that appropriately isolated the

junction gaps between cells. We then calculated the gap areas and sizes of the cell edges presenting discontinuous and break junctions. The average size of gap area per 100 μm^2 represents the inter-endothelial gap area value in each image.

Mouse Inflammation Cytokine Array. Sera were collected to analyze systemic cytokine expression profile using Mouse inflammation Cytokine Array C (133999, Abcam), which can detect 40 cytokines. The detailed procedures of cytokine array experiments were previously described.[7] Briefly, cytokine antibody array membranes were blocked with 5% BSA/TBS (0.01 M Tris–HCl pH 7.6/0.15 M NaCl) for 1 h. Membranes were then incubated with about 100 μL of mouse serum overnight at 4°C. After extensive washing with TBS/0.1% Tween 20 (three times, 5 min each) and TBS (two times, 5 min each) to remove unbounded materials, the membranes were incubated with a cocktail of biotin-labeled antibodies against different individual cytokines. The membranes were then washed and incubated with HRP-conjugated streptavidin (2.5 pg/mL) for 1 h at room temperature. Unbound HRP-streptavidin was washed out with TBS/0.1% Tween 20 and TBS. The chemiluminescent signals and the relative cytokine intensities were detected and quantified using VisionWorks LS6.3.3 (UVP). Each spot was corrected for adjacent background intensity and normalized to the membrane's positive controls. Each specimen was measured in duplicate, and the mean signal intensity value for each cytokine within a specimen was determined.

Atherosclerotic Lesion Analysis. Methods for quantifying atherosclerotic lesions were the same as those previously described.[4] After perfusion with 10% zinc-formalin, the heart's upper half containing the aortic root and aorta was dissected and washed overnight in saline at 4°C. The aorta was opened longitudinally using microscissors and pinned flat on a black wax surface for Oil-red O staining. The *en-face* preparation was fixed overnight, washed with

tap water for 10 min, rinsed with 60% isopropanol for 3 min, and placed into 0.5% Oil-red O (#1320-06-5, Sigma-Aldrich) for 15 min at room temperature. After incubation, aortas were washed with 60% isopropanol. Images were taken using a digital camera mounted on the dissecting microscope and were quantified for percent lesion area using Image J software.

Evaluation of Plaque Composition and EC Apoptosis. $_{EC}Vcl^{S721A}ApoE^{-/-}$ and inbred control $ApoE^{-/-}$ mice were fed an HCD for 18 weeks. In some experiments, $ApoE^{-/-}$ mice were intravenously injected with GRK2 inhibitor or saline control and fed an HCD for 18 weeks. Segments of the aortic arch with atherosclerotic plaques were collected to analyze plaque composition and endothelium apoptosis. The plaques in each section were independently assessed by two independent investigators blinded to the study protocol. Specifically, (1) collagen content in plaques was analyzed by PicroSirius red staining (TASS08-125, Toson technology, Hsinchu, Taiwan). The stained areas were automatically detected with Image J software, and the cross-sectional areas of the intima were drawn manually. (2) Synthetic SMC content was examined by co-immunohistochemical staining for αSMA and vimentin (Vim) and calculated as the ratio of immunostained area to total intima area. (3) Fibrous cap thickness was analyzed by Movat pentachrome staining (ab245884, Abcam), and the thin fibrous cap was defined as ≤3 cell layers. The size of necrotic cores was determined by areas lacking DAPI-positive nuclei and drawn manually. (4) Cell apoptosis in lesions was analyzed by TUNEL assay after proteinase K treatment, using the *In Situ* Cell Death Detection Kit (4826-30-K, Trevigen, Gaithersburg, MD, USA). Nuclei were counterstained with DAPI for 5 min. Co-immunostaining was performed to identify ECs undergoing apoptosis by combining TUNEL assay and immunohistochemical staining for vWF. Results were calculated as areas of staining/total intima area. The total intimal lesion area was quantified by averaging six sections spaced 30 μm apart, starting from the base of the aortic root.

***In Vivo* Vascular Permeability Assay.** The detailed procedures of *in vivo* vascular permeability assay were previously described.[8] Briefly, at the end of HCD feeding, Evans blue dye (30 mg/kg in 100 μl PBS; #31413-6, Sigma) was injected into the tail veins of *ApoE*$^{-/-}$ mice or Tg mice with an insulin needle at a rate of 0.01 ml/g of animal weight. Once injected, the needle was removed, and the injection site was pressed with cotton to stop the bleeding. Thirty min after Evans blue dye injection, the mice were euthanized by CO_2 inhalation and perfused with saline. Perfusion completion was confirmed by the uniform clearing of blood from the trachea and other organs. The aorta arch was quickly removed, and the samples were immersed in a plastic tube with 4ºC 4% Zn^{2+}-formalin solution for 2 h. The aorta arches were removed, weighed, and incubated in 1 ml of formamide overnight (or 2 d) at 55°C. Evans blue dye was extracted from the aortic arch with formamide and measured spectrophotometrically at 600 nm using a microplate reader (Infinite® M200, Tecan Trading AG, Switzerland). In one group of experiments, vascular permeability was evaluated by extracting Evans blue dye from sections of normal arteries with equal weights. The dilutions for the standard curve were prepared by diluting Evans blue in the formamide solution in exponential concentrations. The standard concentrations were 0, 1, 2, 4, 8, 16, 32, 64, and 128 μg/ml and were adjusted to the level required for sample absorbance.

***In Vivo* Endothelial Permeability Assay.** The method was modified from McDonald DM.[9,10] Sites aortic arch leakage were marked by extravasated fluorescent polymer microspheres ranging in diameter from 100-nm (20 μl *i.v.;* G100, Duke Scientific, Fremont, CA, USA). Mice received an intravenous injection of 2 ml/kg 100-nm microspheres for 45 min; then, intravascular microspheres were removed from the bloodstream by vascular perfusion of 1% PFA in PBS. The aorta arch was removed and fixed for an additional 2 h, and

the *en-face* vessels were stained for VE-cadherin immune reactivity. The area density of extravasated microspheres in the endothelium (proportion of total pixels) was measured on digital images of different aorta regions. An average area density value was calculated for all images from each mouse.

Diseased Human Coronary Arteries. Thirty diseased human coronary arteries and 12 control internal thoracic arteries were harvested from 35 patients with end-stage heart failure undergoing heart transplantation at Tri-Service General Hospital in Taipei. This protocol was approved by the Hospital Human Subjects Review Committee (approval number TSGHIRB-210305132) and carried out following The Code of Ethics of the World Medical Association (Declaration of Helsinki). The resected samples were fixed and embedded in paraffin blocks. These diseased arteries represented stages of atherosclerosis, from mild lesions with fatty streaks to advanced lesions, according to American Heart Association guidelines for histological classification of atherosclerotic lesions.[11]

Serum from Human Patient Population. The patient specimens (sera) and backgrounds were obtained from Kaohsiung Municipal Siaogang Hospital (KMSH, Taiwan). The study flow chart is shown in *Figure S13*. Informed consent was obtained from each patient before collection. Clinical parameters and pathological features were certified by KMSH (*Table S4*). The extent of CAD was determined according to traditional vessel disease classification, and the Coronary Artery Disease Prognostic Index was performed as previously described.[12] The use of patient serum with different CAD stages and non-CAD normal persons (as controls) in this study was approved by the Institutional Review Board of the National Health Research Institutes (NHRI-IRB-EC1050710-E). The human study was carried out following The Code of Ethics of the World Medical Association (Declaration of Helsinki). Briefly, patients were

recruited to participate in a prospective randomized disease management study. Serum samples for biomarker analysis were obtained from 136 patients with CAD (including 89 patients with mild CAD and 47 patients with moderate or severe CAD) and 26 non-CAD participants who matched the rest of the study population in terms of baseline characteristics. Blood sampling was performed before discharge, and samples were immediately stored at −80°C until the analysis was performed.

Serum Sample Preparation and Analysis. According to the manufacturer's directions, serum VCL and VCL^{S721p} levels were measured using the Human VCL ELISA kit (OKEH01312, AVIVA Systems Biology, San Diego, CA, USA) and the Human IgG ELISA Quantitation Set (E80-104, Bethyl Lab, Montgomery, TX, USA). ELISAs were performed using full-length human VCL protein and VCL^{S721p} polypeptides or a positive standard curve. To detect VCL^{S721p}, ELISAs were performed by our specific rabbit polyclonal antibody against phosphor-serine at residue 721 on VCL. The detailed procedures of analysis were previously described.[13] Briefly, 50 µl of serially diluted standards and 5-fold-diluted patient sera (10 µl serum: 40 µl sample diluents) were added to plates pre-coated with VCL or VCL^{S721p} antibodies first and were then incubated for 30 min at 37°C. After five washes with the diluted buffer concentrate reagent, 50 µl of VCL or VCL^{S721p} antibody conjugated to horseradish peroxidase was added to all wells except blank wells. After incubation for 30 min at 37°C and five washes, 50 µl of substrate A followed by 50 µl of substrate B were added to each well and incubated for 15 min at 37°C. After this, stop solution was added to each well. Absorbance was measured within 15 min of stop solution addition at 450 nm using a microplate reader (Infinite® M200, Tecan Trading AG, Switzerland).

Isolation of Extracellular Vesicles (EVs) and Exosomes from Serum. Mouse serum

samples were filtered through a 0.22 μm RNA/DNA-free syringe filter and processed for exosome isolation. EV fractions were isolated from 0.1 mL of serum by ExoQuick™ Exosome Precipitation Solution according to the manufacturer's instructions (System Biosciences). Briefly, 1/4 volume of ExoQuick solution was added to serum, and the samples were refrigerated at 4 °C overnight. The mixture was centrifuged at 1500×g for 30 min, and the supernatant was removed by aspiration. The pellet fraction as EVs was re-suspended in nuclease-free water. We used 50 μg of EVs from serum as the antigen source, and exosomes were isolated using antibody-conjugated magnetic microbeads. The antibody-conjugated magnetic microbeads were prepared with the Exo-Flow Purification Kit according to the protocols supplied by the manufacturers. Microbeads were washed three times with ice-cold PBS and suspended in RIPA buffer containing the protease inhibitor cocktail. The resultant supernatants containing CD9-positive exosomes were used for Western blot analysis. The isolated EVs and exosomes were quantified using the ExoCET exosome quantification kit according to the manufacturer's protocol.

Statistical Analysis. Continuous data were assessed distribution normality using the Kolmogorov-Smirnov test or Shapiro-Wilk test and analyzed using the appropriate parametric or non-parametric tests described in each figure legend. Normally distributed variables were analyzed by parametric tests and reported as means ± SEM; non-normally distributed variables were analyzed by non-parametric tests and reported as medians and the 25^{th} and 75^{th} quartiles. A two-tailed Student *t*-test or one-way ANOVA with Tukey multiple comparison test was used for all parametric tests. For non-parametric tests, the Mann–Whitney U-test or Kruskal–Wallis test with Dunn multiple comparison tests was applied. Repeated measures data were analyzed by parametric test using two-way ANOVA followed by Tukey multiple comparison test. To analyze the cross-sectional correlation between the

results of staining intensity and the number of macrophages, Spearman's rho correlation test was used. Statistical analysis of the results of *in vitro* cellular and *in vivo* animal experiments was performed using GraphPad Prism Software (version 7). The heterogeneity in demographic and lifestyle variables between CAD and non-CAD groups was compared using the chi-square test for categorical data. Since serum VCL^{S721p} and VCL concentrations were right-skewed, natural log-transformation (ln-transformed) was performed on these variables before statistical analysis. All statistical data on clinical sera were analyzed using the multivariate linear regression model and adjusted for age, sex, smoking, body mass index, hypertension, diabetes, and hypercholesterolemia. The potential regulatory effects of statins and other drugs on the VCL^{S721p}/VCL association were analyzed using a multivariate linear regression model (SAS version 9.4). A *P* value <0.05 was considered statistically significant.

ONLINE SUPPLEMNENTAL REFERENCES

1. Shih YT, Wang MC, Zhou J, Peng HH, Lee DY, Chiu JJ. Endothelial progenitors promote hepatocarcinoma intrahepatic metastasis through monocyte chemotactic protein-1 induction of microRNA-21. *Gut* 2015;**64**:1132-1147. doi: 10.1136/gutjnl-2013-306302

2. Wang YT, Pan SH, Tsai CF, Kuo TC, Hsu YL, Yen HY, et al. Phosphoproteomics Reveals HMGA1, a CK2 Substrate, as a Drug-Resistant Target in Non-Small Cell Lung Cancer. *Sci Rep* 2017;**7**:44021. doi: 10.1038/srep44021

3. Wei SY, Shih YT, Wu HY,Wang WL, Lee PL, Lee CY, et al. Endothelial Yin Yang 1 Phosphorylation at S118 Induces Atherosclerosis Under Flow. *Circ Res* 2021;**129**:1158-1174. doi: 10.1161/CIRCRESAHA.121.319296

4. Lee DY, Lin TE, Lee CI, Zhou J, Huang YH, Lee PL, et al. MicroRNA-10a is crucial for endothelial response to different flow patterns via interaction of retinoid acid receptors and histone deacetylases. *Proc Natl Acad Sci U S A* 2017;**114**:2072-2077. doi: 10.1073/pnas.1621425114

5. Zhou J, Lee PL, Tsai CS, Lee CI, Yang TL, Chuang HS, et al. Force-specific activation of Smad1/5 regulates vascular endothelial cell cycle progression in response to disturbed flow. *Proc Natl Acad Sci U S A* 2012;**109**:7770-7775. doi: 10.1073/pnas.1205476109

6. Jerkic M, Letarte M. Increased endothelial cell permeability in endoglin-deficient cells. *FASEB J* 2015;**29**:3678-3688. doi: 10.1096/fj.14-269258

7. Shih YT, Wang MC, Peng HH, Chen TF, Chen L, Chang JY, et al. Modulation of chemotactic and pro-inflammatory activities of endothelial progenitor cells by hepatocellular carcinoma. *Cell Signal* 2012;**24**:779-793. doi: 10.1016/j.cellsig.2011.11.013

8. Yang F, Zhang Y, Zhu J, Wang J, Jiang Z, Zhao C, et al. Laminar Flow Protects Vascular Endothelial Tight Junctions and Barrier Function via Maintaining the Expression of Long Non-coding RNA MALAT1. *Front Bioeng Biotechnol* 2020;**8**:647. doi:

10.3389/fbioe.2020.00647

9. McDonald DM. Endothelial gaps and permeability of venules in rat tracheas exposed to inflammatory stimuli. *Am J Physiol* 1994;**266**:L61-83. doi: 10.1152/ajplung.1994.266.1.L61

10. Baffert F, Le T, Thurston G, McDonald DM. Angiopoietin-1 decreases plasma leakage by reducing number and size of endothelial gaps in venules. *Am J Physiol Heart Circ Physiol* 2006;**290**:H107-118. doi: 10.1152/ajpheart.00542.2005

11. Stary HC, Chandler AB, Dinsmore RE, Fuster V, Glagov S, Insull W, Jr., et al. A definition of advanced types of atherosclerotic lesions and a histological classification of atherosclerosis. A report from the Committee on Vascular Lesions of the Council on Arteriosclerosis, American Heart Association. *Arterioscler Thromb Vasc Biol* 1995;**15**:1512-1531. doi: 10.1161/01.atv.15.9.1512

12. Bart BA, Shaw LK, McCants CB, Jr. Fortin DF, Lee KL, Califf RM, et al. Clinical determinants of mortality in patients with angiographically diagnosed ischemic or nonischemic cardiomyopathy. *J Am Coll Cardiol* 1997;**30**:1002-1008. doi: 10.1016/s0735-1097(97)00235-0

13. Youns MM, Abdel Wahab AH, Hassan ZA, Attia MS. Serum talin-1 is a potential novel biomarker for diagnosis of hepatocellular carcinoma in Egyptian patients. *Asian Pac J Cancer Prev* 2013;**14**:3819-3823. doi: 10.7314/apjcp.2013.14.6.3819

Supplementary Table S1. The expression levels of endothelial phosphoproteins were identified by large-scale phosphoproteomics analysis.

Abbreviation	Full name	Peptide sequence	Phosphorylation site(s)	Ratio IA/TA	Ratio IA/OA	Ratio OA/TA
AHSG	Alpha-2-HS-glycoprotein	HSFSGVA[pS]VESASGEAFHVGK	Ser318	1.37±0.12	0.61±0.12	2.34±0.54
AHSG	Alpha-3-HS-glycoprotein	HSFSGVASVE[pS]ASGEAFHVGK	Ser321	1.44±0.51	0.43±0.13	3.89±1.85
AQP1	Aquaporin-1	VWT[pS]GQVEEYDLDGDDINSR	Ser249	0.68±0.14	0.58±0.31	1.56±0.88
AQP1	Aquaporin-1	VWTSGQVEEYDLDGDDIN[pS]R	Ser264	1.26±0.37	0.72±0.13	1.72±0.26
ATP2A2	ATPase sarcoplasmic/endoplasmic reticulum Ca^{2+} transporting 2	EFDELNP[pS]AQR	Ser663	0.89±0.02	1.40±0.13	0.65±0.07
CALCRL	Calcitonin gene-related peptide type 1 receptor	IQFGN[pS]FSHSDALR	Ser412	0.69±0.12	0.88±0.39	1.58±0.34
CALCRL	Calcitonin gene-related peptide type 1 receptor	SA[pS]YTVSTISDGAGYSHDYPSEHLNGK	Ser421	1.65±0.48	1.18±0.28	1.49±0.52
CAST	Calpastatin	K[pS]EPELDLSSIK	Ser306	1.43±0.12*	1.48±0.23	0.97±0.03
CAV2	Caveolin-2	H[pS]GVDYADPK	Ser20	1.73±0.53	1.31±0.09*	1.35±0.47
CAV2	Caveolin-2	ADVQLFMDDDSY[pS]R	Ser23	1.78±0.32*	1.52±0.14*	1.44±0.42
eNOS	Nitric oxide synthase, endothelial	KE[pS]SNTDSAGALGTLR	Ser635	0.56±0.17	1.04±0.38	0.56±0.05
eNOS	Nitric oxide synthase, endothelial	KE[pS]SN[pT]DSAGALGTLR	Ser635, Thr638	0.62±0.26	0.60±0.20	1.10±0.56

eNOS	Nitric oxide synthase, endothelial	RKES[pS]NTDSAGALGTLR	Ser636	0.58±0.18	0.76±0.01	0.76±0.25
eNOS	Nitric oxide synthase, endothelial	KESSN[pT]DSAGALGTLR	Thr638	0.51±0.06	0.99±0.17	0.52±0.50
eNOS	Nitric oxide synthase, endothelial	IR[pT]QSFSLQER	Thr1177	0.59±0.11	0.46±0.14	1.12±0.24
eNOS	Nitric oxide synthase, endothelial	IR[pT]Q[pS]FSLQER	Thr1177, Ser1179	0.65±0.05	0.56±0.08	1.18±0.08
eNOS	Nitric oxide synthase, endothelial	TQ[pS]FSLQER	Ser1179	0.42±0.06	0.57±0.06	0.84±0.17
eNOS	Nitric oxide synthase, endothelial	TQSF[pS]LQER	Ser1181	0.39±0.03	0.98±0.23	0.42±0.09
HSPB1	Heat shock protein beta-1	SP[pS]WDPFR	Ser15	3.79±0.77*	1.13±0.21	3.57±1.26
HSPB1	Heat shock protein beta-1	QL[pS]SGVSEIQQTADR	Ser84	2.47±0.47*	1.62±0.04*	1.52±0.29
LMNA	Lamin-A/C	SGAQASSTPL[pS]PTR	Ser22	1.01±0.16	1.13±0.25	0.96±0.29
LMNA	Lamin-A/C	LRL[pS]PSPTSQR	Ser390	0.07±0.01	0.92±0.08	0.08±0.02
LMNA	Lamin-A/C	LRL[pS]P[pS]PTSQR	Ser390, Ser392	0.59±0.19	0.84±0.16	0.75±0.30
LMNA	Lamin-A/C	[pS]VGGSGGGSFGDNLVTR	Ser628	0.98±0.08	1.27±0.21	1.09±0.32
LMNA	Lamin-A/C	SVGG[pS]GGGSFGDNLVTR	Ser632	1.21±0.23	1.17±0.05	1.09±0.15
MDC1	Mediator of DNA damage checkpoint protein 1	VEEDER[pS]PGVHPGR	Ser494	0.35±0.07	0.47±0.07	0.75±0.12
MDC1	Mediator of DNA damage checkpoint protein 1	TPEPNIPTAPELRPS[pT]PTDQPVAPEPLSR	Thr1284	1.67±0.19	1.12±0.20	1.51±0.14

PECAM1	Platelet endothelial cell adhesion molecule	KADPDLVENRY[pS]R	Ser728	0.40±0.13	0.44±0.13	0.90±0.09
PGRMC1	Progesterone receptor membrane component 1	GDQPAASD[pS]DDDEPPPLPR	Ser56	2.07±1.36	1.69±0.46	1.13±0.45
PGRMC1	Progesterone receptor membrane component 1	EGEEPTV[pY]SDEEEPK	Tyr179	0.37±0.07	1.21±0.43	0.40±0.27
PGRMC1	Progesterone receptor membrane component 1	EGEEPTVY[pS]DEEEPK	Ser180	0.41±0.06	1.69±0.19	0.25±0.06
PPP1R18	Protein phosphatase 1 regulatory subunit 18	SLRPAEPQEQ[pS]PR	Ser219	0.16±0.10	0.37±0.08	0.49±0.33
RPS3	40S ribosomal protein S3	DEILPT[pT]PISEQK	Thr221	1.66±0.52	0.71±0.12	2.23±0.54
TFIP11	Tuftelin-interacting protein 11	GAAEEAELED[pS]DDEEKPVKQDEFPK	Ser89	1.89±0.06	1.31±0.09	1.45±0.11
TFIP11	Tuftelin-interacting protein 11	TTQSLQDFPVVD[pS]EEEAEEEFQK	Ser210	1.71±0.43	1.36±0.16	1.24±0.23
VDAC1	Voltage-dependent anion-selective channel protein 1	LTFDSSF[pS]PNTGKK	Ser104	0.56±0.09	1.05±0.16	0.56±0.16
VDAC2	Voltage-dependent anion-selective channel protein 2	LTFDTTF[pS]PNTGKK	Ser115	1.14±0.08	0.87±0.05	1.31±0.14
VCL	Vinculin	DPTA[pS]PGDAGEQAIR	Ser290	0.45±0.25	1.36±0.21	0.35±0.19
VCL	Vinculin	MTGLVDEAID[pT]KSLLDASEEAIKK	Thr719	0.75±0.53	0.94±0.48	1.24±0.92

VCL	Vinculin	MTGLVDEAIDTK[pS]LLDASEEAIKK	Ser721	2.86±0.30*	1.82±0.18*	1.28±0.06
VTN	Vitronectin	D[pS]WEDIFR	Ser289	1.16±0.66	1.22±0.32	0.96±0.42

Large-scale phosphoproteomics was used to analyze the expression levels of phosphoproteins in the cell lysates of porcine endothelium. Data are presented as the ratio of the expression levels of phosphoproteins in the cell lysates of vascular endothelium in the inner curvature of the aortic arch (IA) to those of the outer curvature of the aortic arch (OA) or thoracic aorta (TA). Data are means ± SEM from three independent experiments and were analyzed by Kruskal–Wallis test with Dunn multiple comparisons test. *$P \leq 0.05$ for up-regulation in IA *vs*. OA or TA.

Supplementary Table S2. Analysis of body weights, serum chemistry, and plasma lipid profiles of $_{EC}Vcl^{S721A}ApoE^{-/-}$ mice fed a normal diet (ND) or a high-cholesterol diet (HCD).

Groups	Mice fed a ND			Mice fed an HCD		
Transgenic ApoE$^{-/-}$ mice	wt/wt	$_{EC}Vcl^{S721A}$/wt	$_{EC}Vcl^{S721A}/_{EC}Vcl^{S721A}$	wt/wt	$_{EC}Vcl^{S721A}$/wt	$_{EC}Vcl^{S721A}/_{EC}Vcl^{S721A}$
Body mass (g)	25.0 ± 0.8	25.1 ± 1.5	25.7 ± 1.1	28.3 ± 0.5*	28.0 ± 0.3*	28.8 ± 1.6*
CPK(m/L)	85.0 ± 2.9	84.7 ± 4.7	87.7 ± 4.1	175.3 ± 10.7*	163.0 ± 1.2*	164.0 ± 7.8*
LDH (m/L)	219.3 ± 14.1	215.0 ± 10.4	222.7 ± 11.0	393.3 ± 31.1*	392.7 ± 6.5*	404.7 ± 9.9*
BUN (mg/dl)	23.4 ± 0.5	25.9 ± 2.0	25.1 ± 1.0	26.3 ± 2.5	28.5 ± 1.1	29.3 ± 1.4
CRE (mg/dl)	0.3 ± 0.0	0.3 ± 0.1	0.3 ± 0.0	0.4 ± 0.0	0.4 ± 0.1	0.4 ± 0.1
TCHO(mg/dL)	513.3 ± 12.7	506.7 ± 35.6	485.0 ± 39.2	852.7 ± 42.4*	796.7 ± 67.1*	741.3 ± 47.1*
HDLC(mg/dL)	91.7 ± 2.5	90.4 ± 5.3	91.0 ± 10.6	136.9 ± 23.7	150.3 ± 28.0	149.0 ± 4.3
TG(mg/dL)	119.3 ± 14.1	115.0 ± 10.4	122.7 ± 11.0	293.3 ± 31.1	292.7 ± 6.5	304.7 ± 9.9
LDLC(mg/dL)	334.2 ± 15.1	340.1 ± 1.0	352.5 ± 68.0	582.1 ± 18.7	551.9 ± 32.2	533.9 ± 54.9

Serum samples of transgenic *ApoE*$^{-/-}$ mice, including inbred control *wt/wt ApoE*$^{-/-}$ mice, heterogeneous $_{EC}Vcl^{S721A}$*/wt ApoE*$^{-/-}$ mice, and homogenous $_{EC}Vcl^{S721A}/_{EC}Vcl^{S721A}$ *ApoE*$^{-/-}$ mice were fed a ND or an HCD for 12 weeks. Data are expressed as means ± SEM from eight independent experiments (n=8 each). HDLC and LDLC were analyzed by Kruskal–Wallis test with Dunn multiple comparisons test, and other data were analyzed by two-way ANOVA with Tukey multiple comparison test. *P<0.05 *vs*. inbred control *wt/wt ApoE*$^{-/-}$ mice. CPK, creatine phosphokinase. LDH, lactic dehydrogenase. BUN, blood urea nitrogen. CRE, creatinine. TCHO, total cholesterol. HDLC, high-density lipoprotein cholesterol. TG, triglyceride. LDLC, low-density lipoprotein cholesterol.

Supplementary Table S3. The effects of a GRK2 inhibitor on the body weights, serum chemistry, and plasma lipid profiles of *ApoE*$^{-/-}$ mice fed a high-cholesterol diet (HCD).

Group	Saline	GRK2 inhibitor
Body mass (g)	29.3 ± 0.6	28.0 ± 0.8
CPK (m/L)	175.3 ± 10.7	163.0 ± 1.2
LDH (m/L)	393.3 ± 31.1	392.7 ± 6.5
BUN (mg/dl)	26.3 ± 2.5	28.5 ± 1.1
CRE (mg/dl)	0.4 ± 0.1	0.4 ± 0.1
TCHO (mg/dL)	927.5 ± 102.3	867.5 ± 82.1
HDLC (mg/dL)	132.3 ± 25.4	140.6 ± 35.6
TG (mg/dL)	184.5 ± 43.9	178.5 ± 43.4
LDLC (mg/dL)	658.4 ± 88.7	633.8 ± 99.9

ApoE$^{-/-}$ mice were fed an HCD and administrated with a GRK2-specific inhibitor (10 mg/kg IV every 3 d) or control saline for 12 weeks, and their sera were analyzed. Data are expressed as means ± SEM from eight independent experiments (n=8 each). HDLC and LDLC were analyzed by the Mann–Whitney test, and other data were analyzed by the two-tailed Student *t*-test. CPK, creatine phosphokinase. LDH, lactic dehydrogenase. BUN, blood urea nitrogen. CRE, creatinine. TCHO, total cholesterol. HDLC, high-density lipoprotein cholesterol. TG, triglyceride. LDLC, low-density lipoprotein cholesterol.

Supplementary Table S4. Clinical characteristics of the study group.

	All subjects	Healthy (Non-CAD)	Mild CAD (index<42)	Moderate /Severe CAD (index≥42)	*p* value
N	162	26	89	47	
Sex (female/male)	26/136	6/20	16/73	4/43	0.5282[a]
Age (yr)	63.0 (56.0-67.0)	59.5 (54.8-66.0)	64.0 (58.5-67.0)	61.0 (55.0-67.0)	0.1381[b]
BMI (kg/m^2)	26.2 (24.2-28.6)	25.2 (22.5-26.5)	26.6 (24.4-28.9)	27.2 (24.6-28.9)*	0.0371[b]
Waist circumference (cm)	92.0 (827.5-98.3)	85.9 (79.8-90.3)	92.0 (89.0-98.5)*	93.0 (88.0-101.0)*	<0.001[b]
SBP (mmHg)	127.8 (114.8-142.0)	121.8 (108.2-128.2)	132.0(115.0-142.0)	131.0 (119.0-145.0)	0.0748[b]
DBP (mmHg)	79.0 (71.8-86.4)	77.6 (73.2-82.6)	80.0 (72.0-87.0)	79.0 (70.0-88.0)	0.8060[b]
Smoking (No/Yes/ex)	54/56/52	15/5/6	29/29/31	10/22/15	0.0218[a]
TCHO (mg/dl)	168.0 (144.3-188.0)	185.5 (167.0-196.5)	158.0 (129.0-182.0)*	171.0 (155.0-186.0)*	0.0003[b]
HDLC (mg/dl)	39.1 (42.6-76.0)	38.6 (36.7-39.5)	39.2 (34.6-43.0)	38.9 (34.4-45.8)	0.6073[b]
LDLC (mg/dl)	94.5 (76.0-115.3)	92.5 (86.0-98.3)	93.0 (68.5-118.0)	102.0 (80.0-125.0)	0.3675[b]
TG (mg/dl)	121.5 (95.0-170.5)	108.5 (98.8-121.5)	122.0 (90.5-168.0)	153.0 (98.0-216.0)*	0.0498[b]
Diabetes	52/162(25.6%)	0/26(0%)	33/89(37.1%)*	19/47(40.4%)*	0.0084[a]
Hypercholesterolemia	59/162(36.4%)	0/26(0%)	40/89 (44.9%)*	19/47 (40.4%)*	0.0001[a]
Hypertension	81/162(50.0%)	5/26 (19.2%)	47/89 (52.8%)*	29/47 (61.7%)*	0.0017[a]
Medication					
Antiplatelets	45/162 (27.8%)	0/26(0%)	24/89 (27.0%)*	21/47 (44.7%)*	0.0002[a]
β-Blockers	29/162(17.9%)	0/26(0%)	13/89(14.6%)*	16/47(34.0%)*#	0.0007[a]
CCBs	13/162(8.0%)	0/26(0%)	7/89(7.9%)	6/47(12.8%)	0.1570[a]
Fibrates	3/162(1.9%)	0/26(0%)	3/89(3.4%)	0/47(0%)	0.2855[a]

Statins	**122/162 (75.3%)**	**0/26(0%)**	**80/89(80.9)***	**42/47(89.4%)***	**<0.0001[a]**
Serum markers					
sVCL^{S721p} (ng/ml)	**32.8(21.4-47.2)**	**21.8(13.2-26.2)**	**32.4(20.2-49.7)***	**38.8(31.2-51.6)*#**	**<0.0001[b]**
sVCL (ng/ml)	**49.8(34.5-77.2)**	**27.6(18.2-39.8)**	**54.0(37.4-87.9)***	**58.0(44.5-80.5)***	**<0.0001[b]**

Results are expressed as the Median (interquartile range) from CAD patients and healthy subjects. Antiplatelet drugs include Aspirin, Brilinta, Pleraal and Plavix. β-blockers include Concor, Kerlone, Inderal and Tenormin. Calcium channel blockers (CCBs) include Amlodipine, Amtrel, Exforge, and Norvasc. Fibrates include Bezafibrate, Clofibrate, Fenolip and Gemfibrozil. Statins include Crestor, Caduet, Lipitor and Vytorin. Data were analyzed by chi-square test, Kruskal–Wallis test with Dunn multiple comparisons test. A P value≤0.05 was considered significantly different for CAD *vs.* non-CAD groups*, mild CAD *vs.* moderate/severe CAD groups[#]. BMI, body mass index. SPB, systolic blood pressure. DBP, diastolic blood pressure. TCHO, total cholesterol. HDLC, high-density lipoprotein cholesterol. LDLC, low-density lipoprotein cholesterol. TG, triglyceride.

ONLINE SUPPLEMENTARY FIGURES

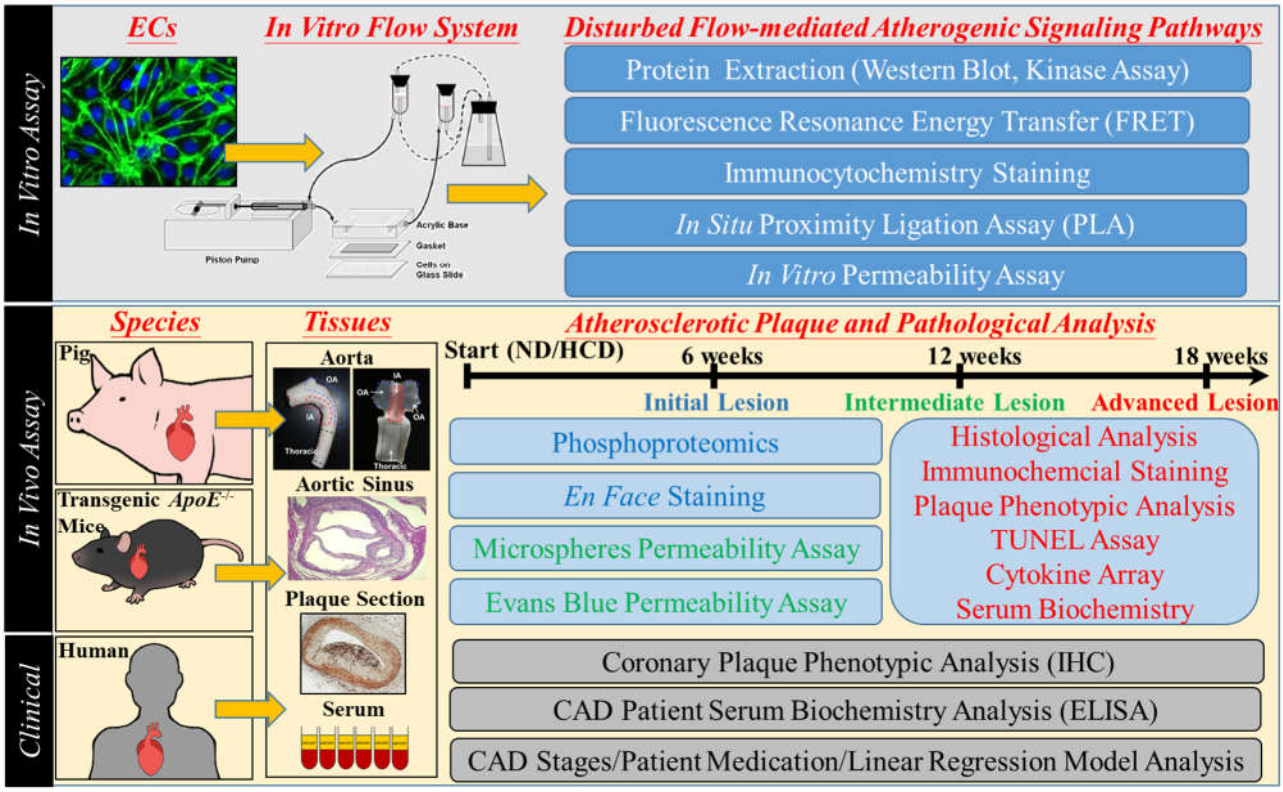

Supplementary Figure S1. Experimental workflow of the study. A flowchart summarizes the combination of *in vitro* flow system, experimental animal models, and human specimens and their experimental procedures to discover a novel endothelial atherogenic phosphoprotein, i.e., VCL^{S721p}, induced by disturbed flow to promote endothelial permeability and atherosclerosis development. ND, normal diet. HCD, high-cholesterol diet. IHC, immunohistochemistry. ELISA, enzyme-linked immunosorbent assay.

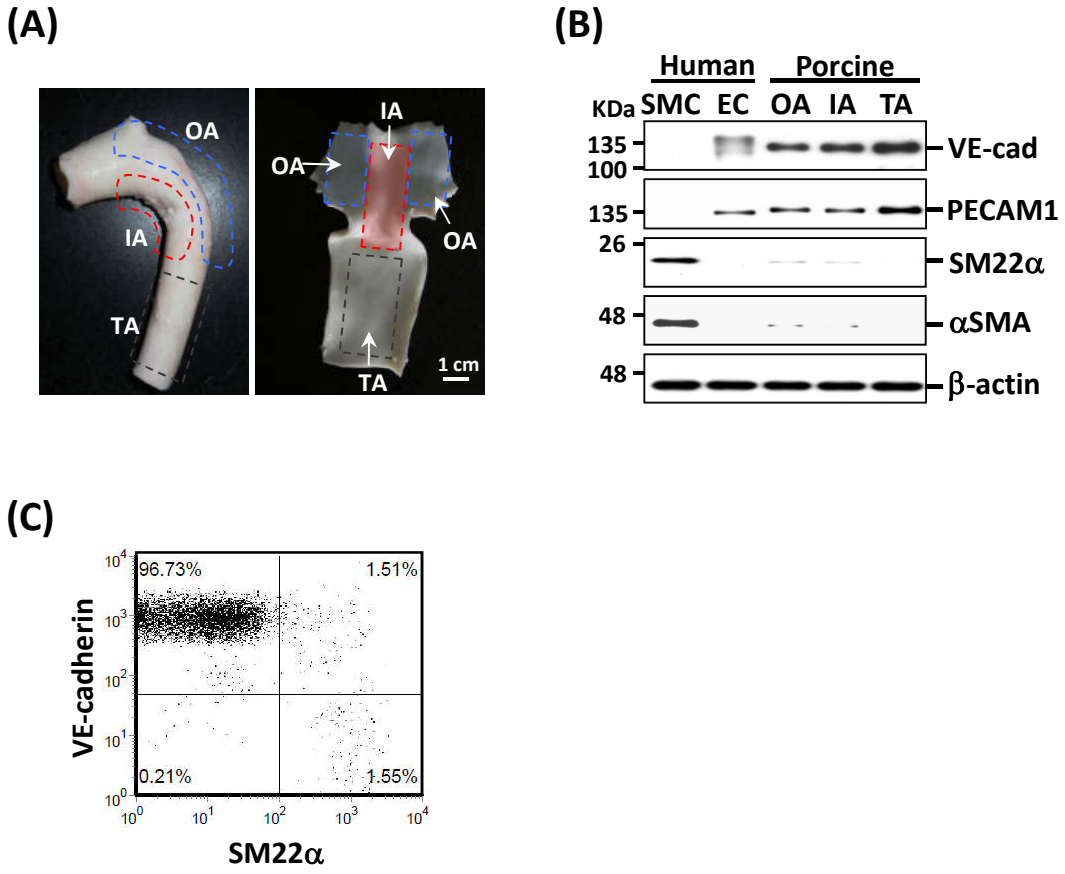

Supplementary Figure S2. Characterization of scraped porcine ECs. (*A*) Illustration of the regions where ECs were harvested in the porcine aorta and endothelial lumen. **(*B* and *C*)** Representative data of Western blot **(*B*)** and flow cytometry **(*C*)** analyses of scraped porcine ECs for EC (VE-cadherin and PECAM1) and SMC (SM22α and αSMA) markers. Human aortic ECs and SMCs were used as controls. The EC purity (i.e., VE-cadherin^{+}/SM22α^{-} cells) was characterized as >96%, with low SMC contamination. IA, inner curvature of the aortic arch. OA, outer curvature of the aortic arch. TA, thoracic aorta.

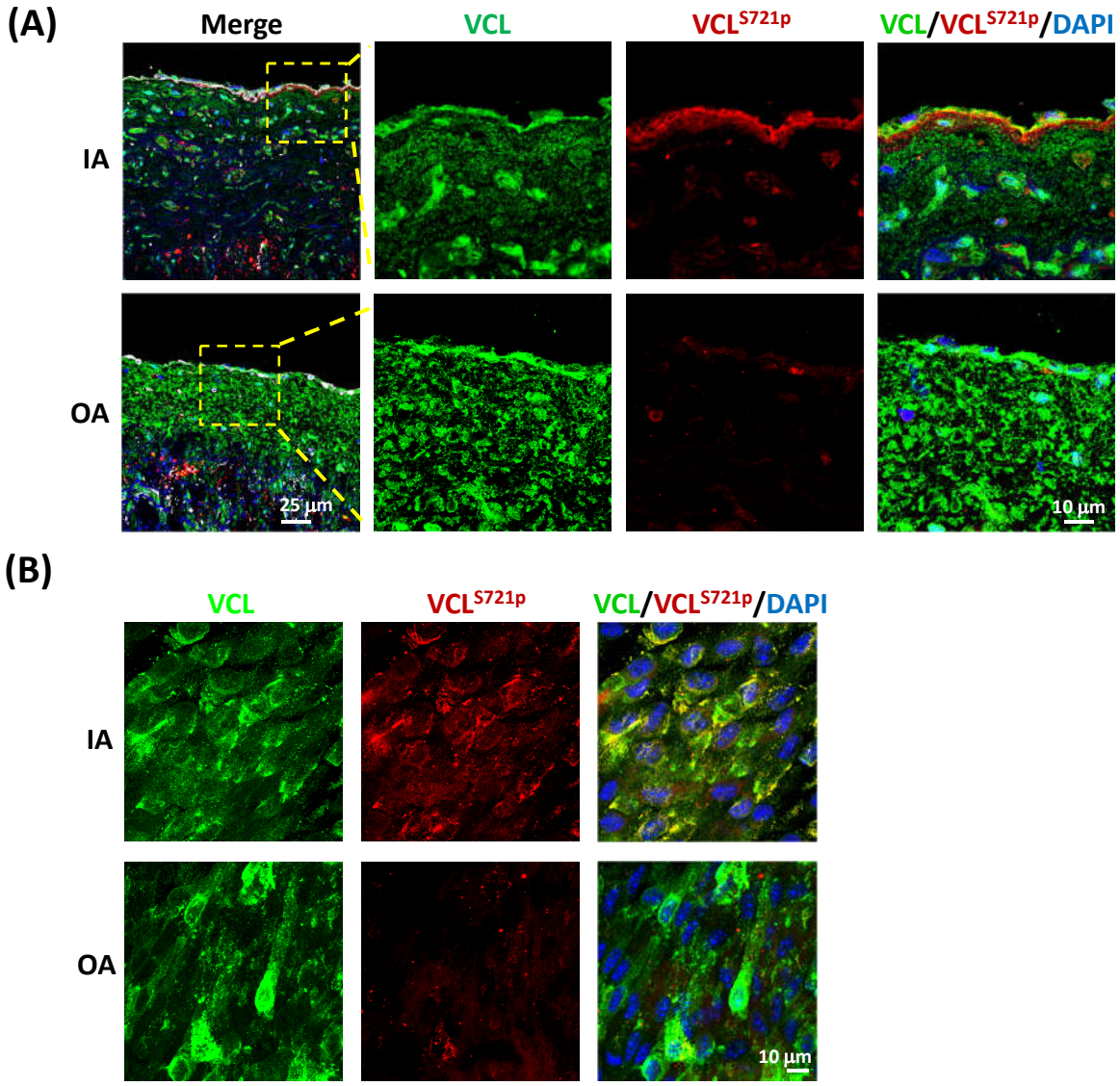

Supplementary Figure S3. Representative photomicrographs of immunohistochemical staining for VCL and VCL^{S721p} in porcine and *ApoE*$^{-/-}$ mouse aortic arches. (*A*) Serial cross-sections of the inner curvature (IA) and outer curvature (OA) of the porcine aortic arch were immunostained for VCL (green), VCL^{S721p} (red), and EC marker IB4 (white) to examine VCL and VCL^{S721p} expressions in porcine ECs. The right panels are the magnified views of the indicated areas (yellow dashed line box) in the left panels. **(*B*)** Representative images of *en-face* co-immunostaining for VCL and VCL^{S721p} in the endothelium of the IA and OA of *ApoE*$^{-/-}$ mice fed an HCD for 6 weeks. Cell nuclei were counterstained with DAPI. The pictured images represent three independent experiments with similar results.

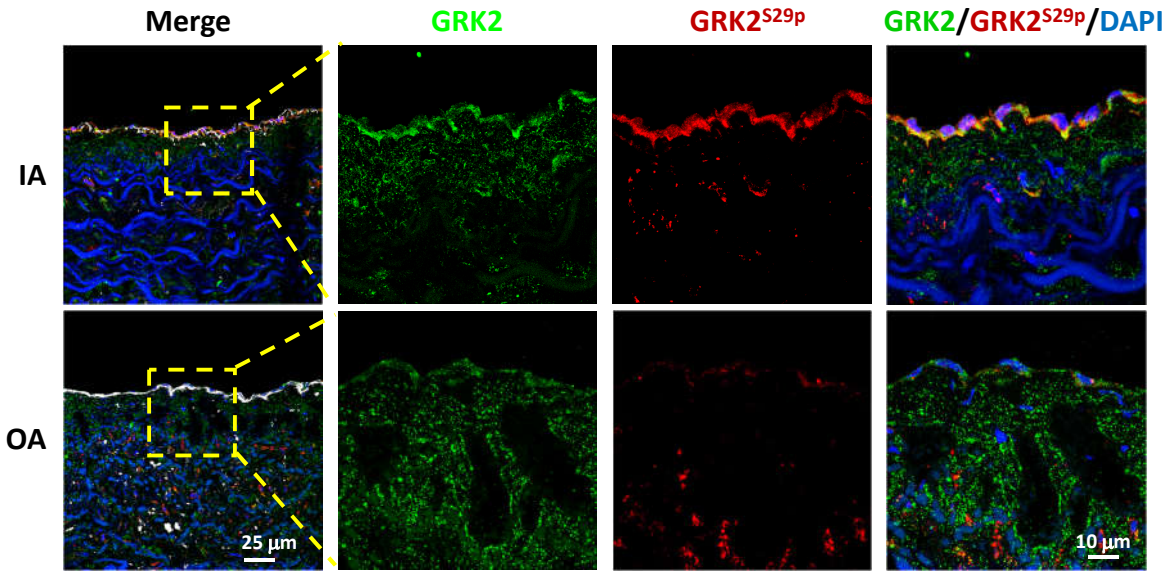

Supplementary Figure S4. Representative photomicrographs of immunohistochemical staining for GRK2 and GRK2^{S29p} in the IA and OA of the porcine aortic arch. Cross-sections of the inner (IA) and outer curvatures (OA) of the porcine aortic arch were immunostained for GRK2 (green), GRK2^{S29p} (red), and EC marker IB4 (white) to examine the GRK2 and GRK2^{S29p} expressions in porcine ECs. Cell nuclei were counterstained with DAPI. The right panels are the magnified views of the indicated areas (yellow dashed line box) in the left panels. The pictured images represent three independent experiments with similar results.

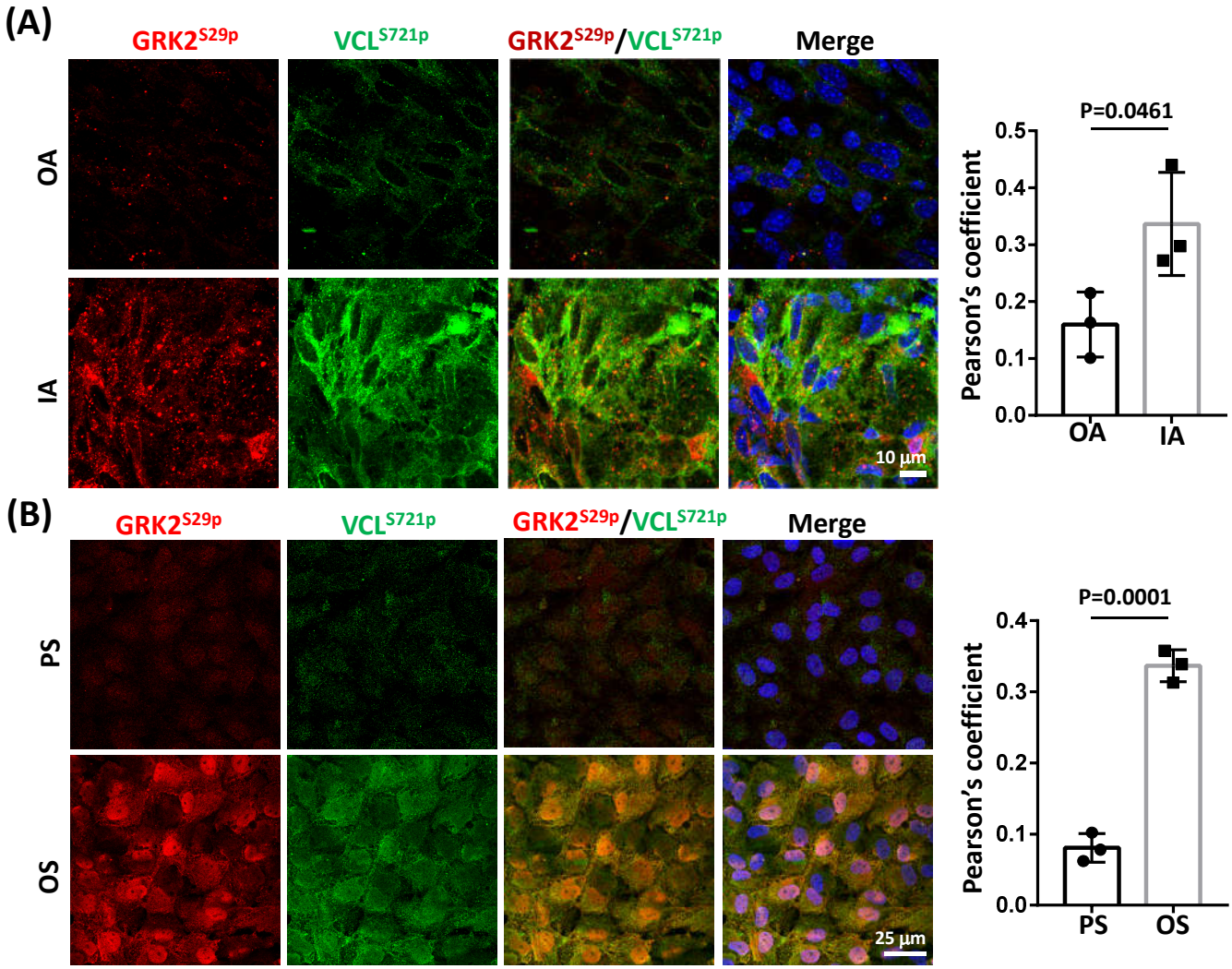

Supplementary Figure S5. Co-localization of GRK2^{S29p} and VCL^{S721p} in ECs exposed to disturbed flow *in vitro* and in athero-susceptible endothelium of *ApoE*$^{-/-}$ mice. (*A*) Representative images of *en-face* co-immunostaining for GRK2^{S29p} (red) and VCL^{S721p} (green) in the endothelium of IA and OA in *ApoE*$^{-/-}$ mice fed an HCD for 6 weeks. **(*B*)** Cultured ECs were subjected to oscillatory (OS) or pulsatile (PS) shear stress for 24 h. The co-localization of GRK2^{S29p} with VCL^{S721p} in ECs was examined by co-immunostaining with anti-VCL^{S721p} antibody conjugated with Alexa Fluor 488 (green) and anti-GRK2^{S29p} antibody conjugated with Alexa Fluor 594 (red). Cell nuclei were counterstained with DAPI. Data in ***A*** and ***B*** were means±SEM (n=3). Quantitative analysis of overlapping red and green channel pixels was validated by Pearson's correlation coefficient (Image J). The pictured images represent three independent experiments with similar results.

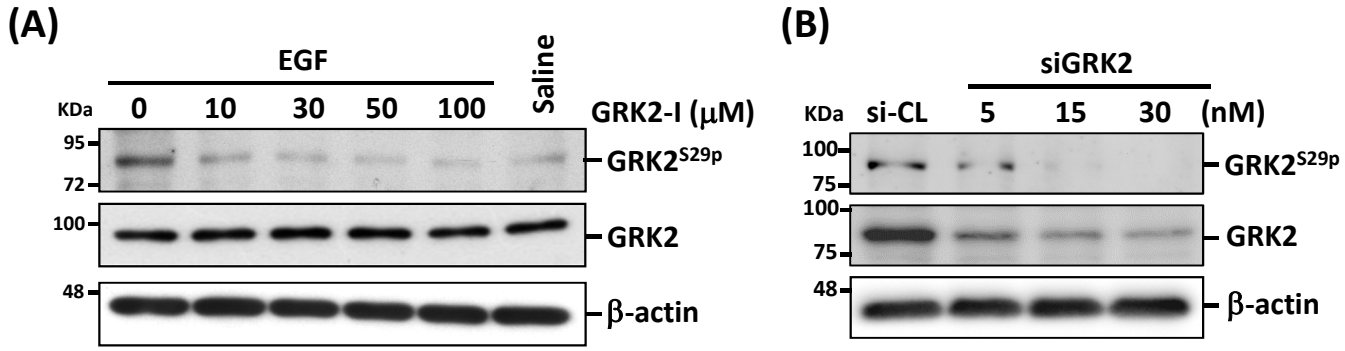

Supplementary Figure S6. Efficacy of the GRK2-specific inhibitor and siRNA in the blockage of GRK2 activation and expression in ECs. (*A*) ECs were pre-treated with the indicated concentration of GRK2 inhibitor (GRK2-I) for 1 h, and the activation of GRK2 (i.e., $GRK2^{S29p}$) in ECs stimulated with EGF (100 ng/mL, 1 h) was determined by Western blot analysis. **(*B*)** ECs were transfected with control siRNA (siCL) and GRK2-specific siRNA (siGRK2) at the indicated concentrations for 1 d, and the expressions of GRK2 and GRK^{S29p} were examined. Results represent three independent experiments with similar results.

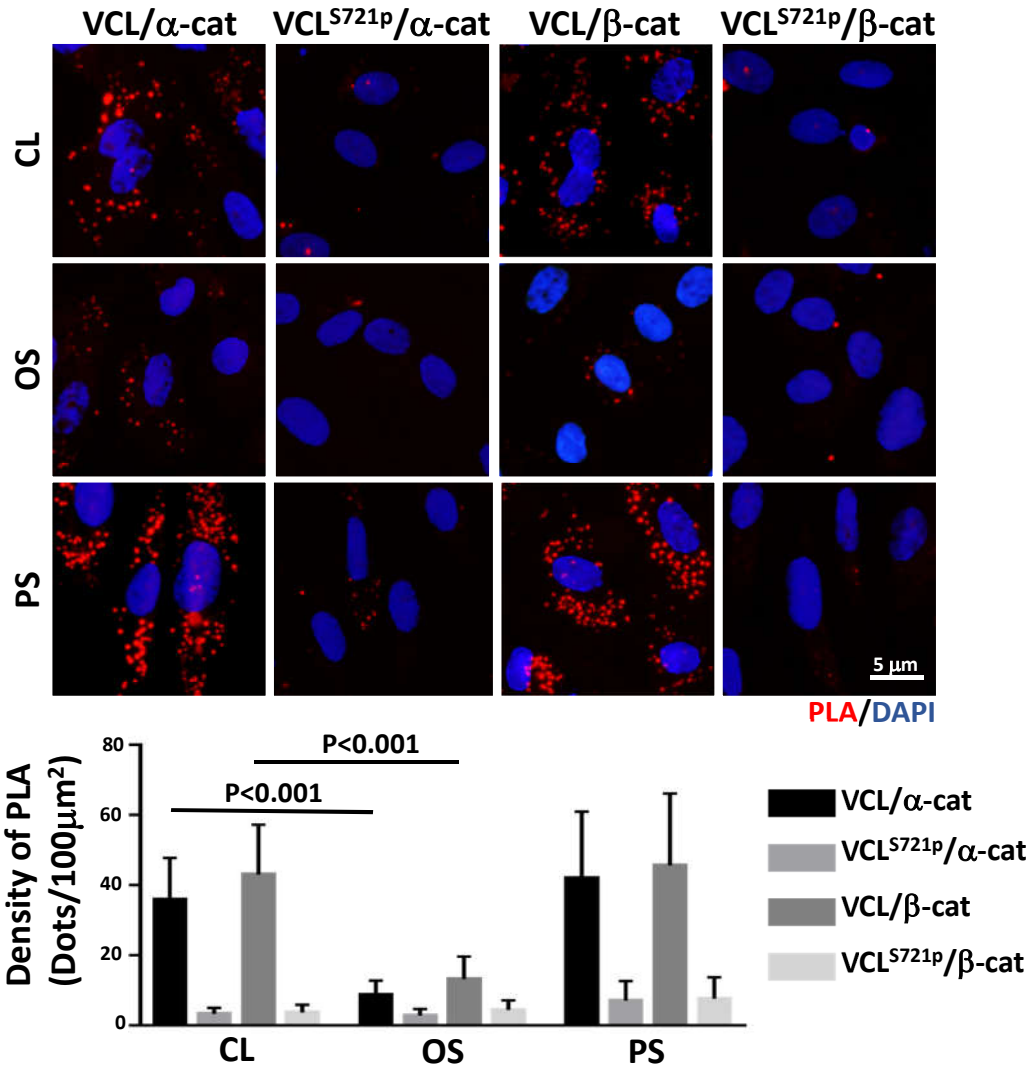

Supplementary Figure S7. Disturbed flow inhibits the associations of VCL with α- and β-catenin in ECs. Cultured ECs were kept under static condition as controls (CL) or subjected to oscillatory (OS) and pulsatile (PS) shear stress for 24 h. The associations of VCL and VCL^{S721p} with α-catenin and β-catenin in ECs were examined by *in situ* PLA. Cell nuclei were counterstained with DAPI. The positive PLA signals were exhibited as red dots, and the density of PLA was quantified. Data are means±SEM from three independent experiments and were analyzed using one-way ANOVA with Tukey multiple comparison text. Images in each picture represent three independent experiments with similar results.

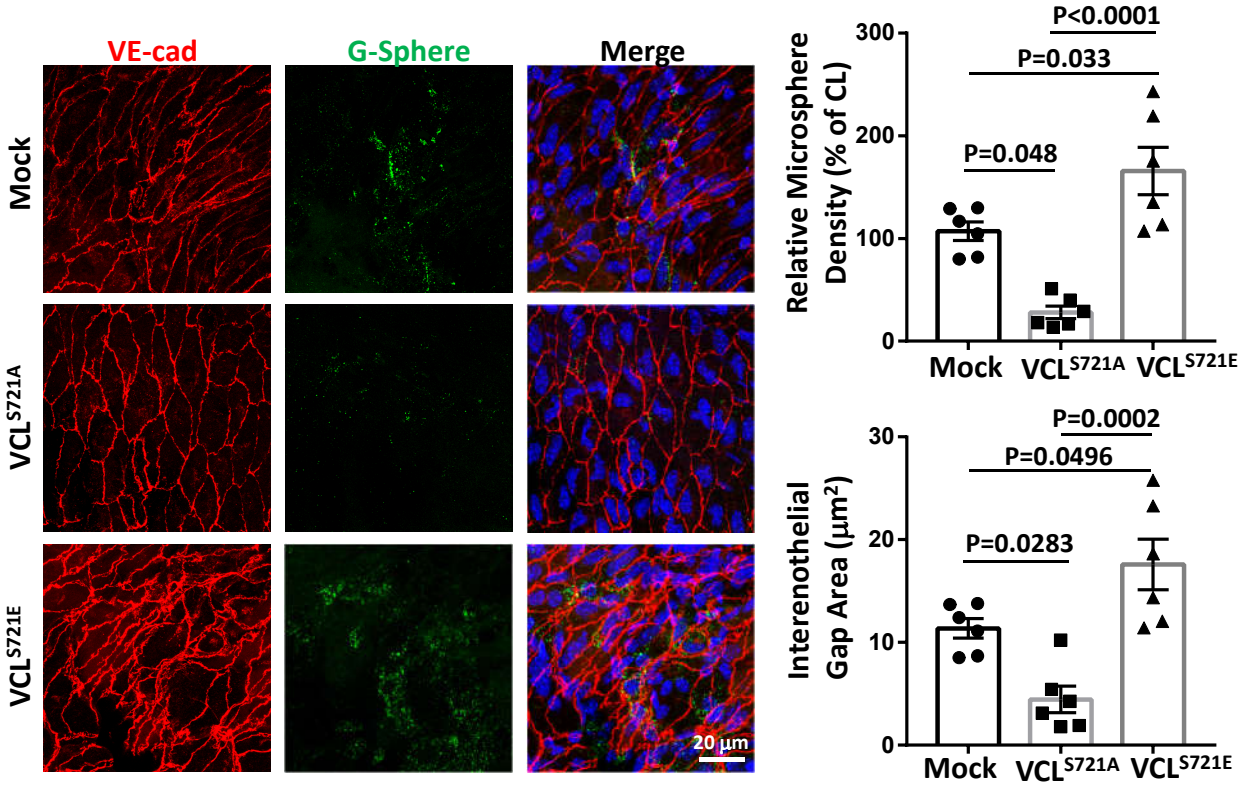

Supplementary Figure S8. Overexpression of VCL^{S721A} and VCL^{S721E} regulate endothelial permeability *in vivo*. *ApoE*$^{-/-}$ mice (6 weeks old, fed HCD) were administrated with VCL^{S721A}, VCL^{S721E}, or mock control (2 μg DNA/g, IV, every 3 d) *via* intravenous injection by *in vivo* Turbofect Reagent for 6 weeks, and the *in vivo* endothelial permeability assay was performed using microsphere extravasation as a readout. *En-face* immunostaining was performed on the endothelium in the IA for VE-cadherin (red) and FITC-conjugated microspheres (G-spheres, 0.1 μm in size, green). Cell nuclei were counterstained with DAPI. The inter-endothelial gap areas and the leakage intensity of G-spheres were quantified. Data are means±SEM (n=6) and were analyzed using one-way ANOVA with Tukey multiple comparison test.

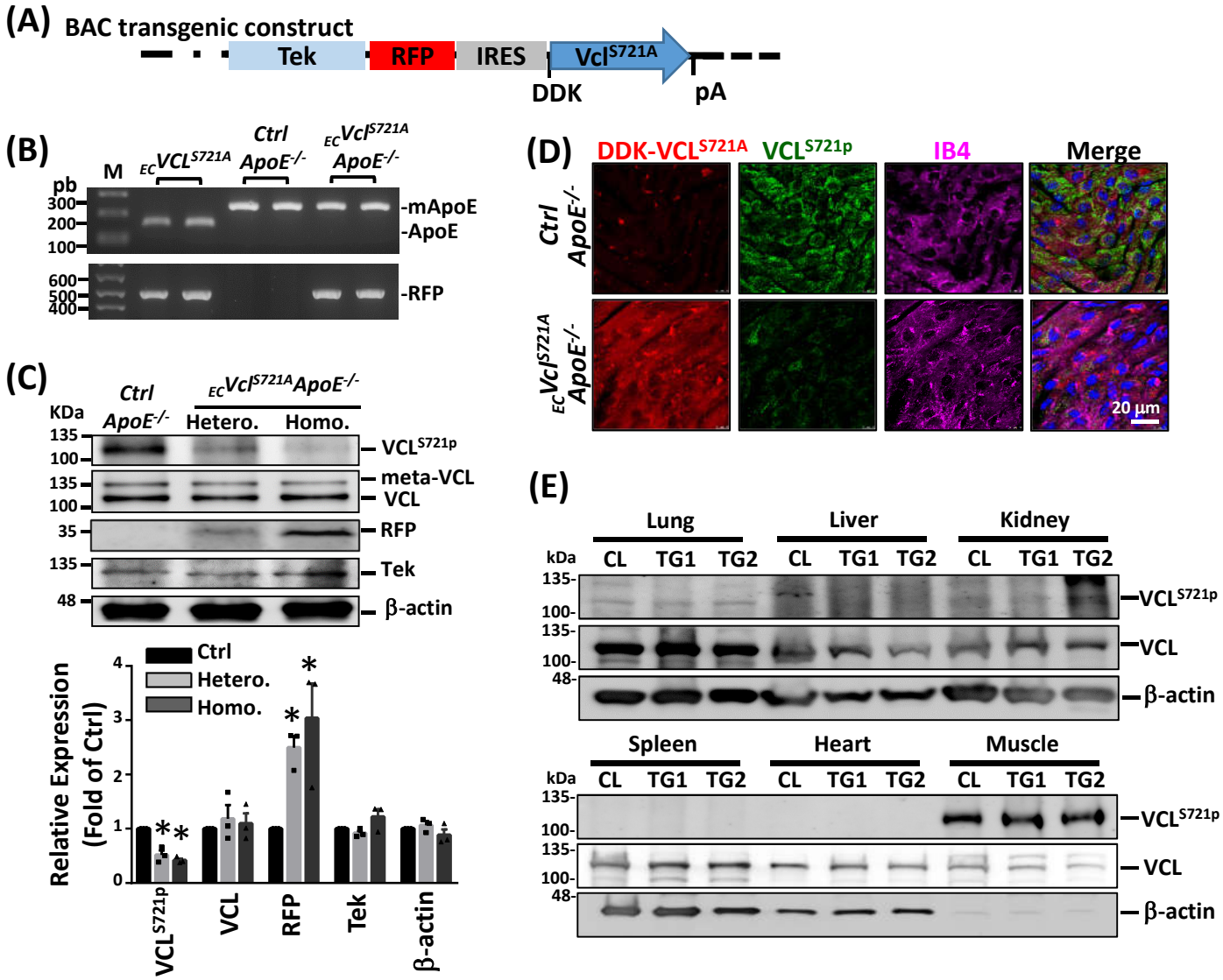

Supplementary Figure S9. Generation and characterization of BAC-based $_{EC}Vcl^{S721A}$ Tg *ApoE*$^{-/-}$ mice. (***A***) Schematic diagram of the EC-specific VCL^{S721A} construct based on the BAC system. The mTek-driven RFP and point-mutant VCL^{S721A} gene were inserted immediately after the start codon of the endothelial-specific Tek promoter (also known as Tie2) in a BAC transgenic construct. The mTek-RFP-IRES-DDK-VCL^{S721A}-polyA- expressing cassette on a BAC construct was used to generate EC-specific *Vcl*^{S721A} Tg *ApoE*$^{-/-}$ mice. **(*B*)** Representative PCR genotyping of founder $_{EC}Vcl^{S721A}$ Tg *ApoE*$^{-/-}$ mice. Screening of mutated ApoE (mApoE, i.e., *ApoE*$^{-/-}$) and RFP was positive for $_{EC}Vcl^{S721A}$ Tg *ApoE*$^{-/-}$ mouse lines. **(*C*)** Western blot analysis of aortic tissue extracts for VCL^{S721p}, VCL, meta-VCL (VCL splice isoform in SMCs), tagged protein RFP, and endothelial marker Tek in heterogeneous $_{EC}Vcl^{S721A}$/*wt ApoE*$^{-/-}$ and homogenous $_{EC}Vcl^{S721A}$/$_{EC}Vcl^{S721A}$ *ApoE*$^{-/-}$ mice fed a normal diet for 6 weeks, as compared with inbred control (*wt/wt*) *ApoE*$^{-/-}$ mice (n=3 each). Data are means±SEM and were analyzed by one-way ANOVA with Tukey multiple comparison test. *P<0.01 *vs*. Ctrl *ApoE*$^{-/-}$ group. **(*D*)** Representative images of *en-face* staining for DDK-tagged VCL^{S721A} (red), VCL^{S721p} (green), and EC marker IB4 (purple) in the endothelium of IA in $_{EC}Vcl^{S721A}$ Tg *ApoE*$^{-/-}$ mice compared to inbred control *ApoE*$^{-/-}$ mice. **(*E*)** Inbred control *ApoE*$^{-/-}$ (CL) and $_{EC}Vcl^{S721A}$ Tg *ApoE*$^{-/-}$mice were fed an HCD for 6 weeks. We collected the total aorta and other tissues—including lung, liver, kidney, spleen, heart, and skeletal muscle—of these mice; the expressions of VCL^{S721p} and total VCL in these tissues were examined by Western blot analysis. The pictured images represent two to three independent experiments with similar results.

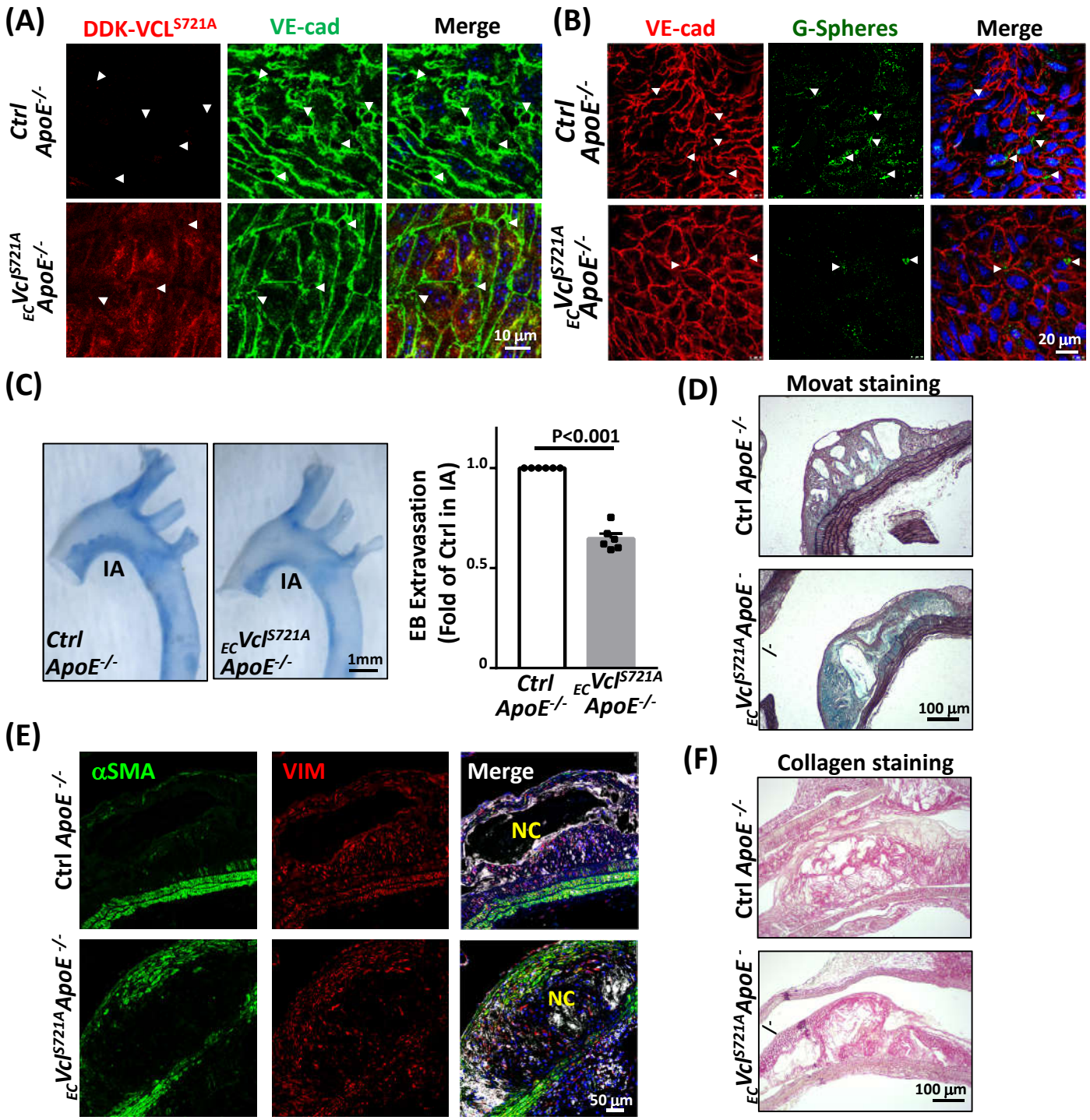

Supplementary Figure S10. EC-specific overexpression of non-phosphorylatable VCL^{S721A} reduces endothelial and vascular permeabilities and regulates atherosclerotic plaque phenotype in $_{EC}Vcl^{S721A}ApoE^{-/-}$ mice. $_{EC}Vcl^{S721A}ApoE^{-/-}$ and inbred control *ApoE*$^{-/-}$ mice were fed an HCD for 6 weeks (***A-C***) and 18 weeks (***D-F***) (n=6 each). (***A***) The endothelia of the IA region were subjected to *en-face* co-immunostaining for DDK-tagged VCL^{S721A} and VE-cadherin. (***B*** and ***C***) These mice were subjected to *in vivo* endothelial (***B***) or vascular (***C***) permeability assay using FITC-conjugated microspheres (G-spheres, 0.1 μm in size, green) or Evans blue (EB). Arrowheads indicate the inter-endothelial gaps between VE-cadherin junctions (***A***) and the leakage site for G-spheres (***B***). Whole segments of mouse aortas were subjected to EB staining to examine dye leakage in these mice (***C***). Quantitative data of the results in ***A*** and ***B*** are shown in *Figures 5A* and *5B*, respectively. (***D-F***) Representative photomicrographs of Movat pentachrome staining (***D***), co-immunohistochemical staining for αSMA and vimentin (Vim) (***E***), and picrosirius red staining (***F***) in aortic lesions. NC, necrotic core. All analyses in ***D-F*** were performed on the sections of the innominate artery and the IA region of mice, and quantitative data of the results are shown in *Figures 5E-5H*. Results represent at least three independent experiments with similar results.

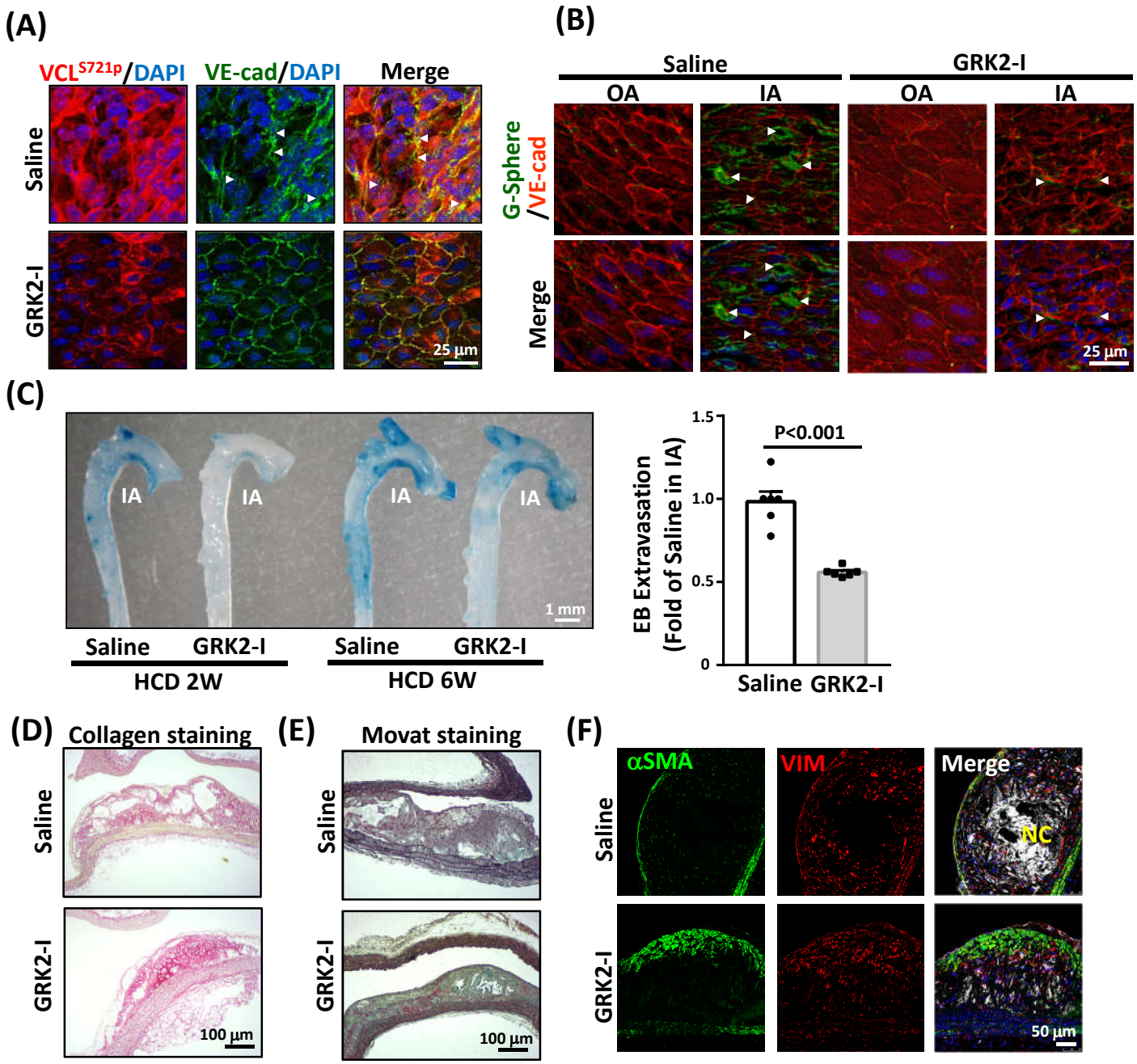

Supplementary Figure S11. GRK2 inhibitor reduces endothelial and vascular permeabilities and increases plaque stability in *ApoE*$^{-/-}$ mice. *ApoE*$^{-/-}$ mice received vehicle control or GRK2-specific inhibitor (GRK2-I, 10 mg/kg IV every 3 d) for 6 **(*A*-*C*)** and 18 **(*D*-*F*)** weeks. **(*A*)** *En-face* immunofluorescence micrographs of the endothelium in the IA co-immunostained for VCL^{S721p} and VE-cadherin with DAPI nuclear counterstains (n=6). **(*B* and *C*)** These mice were subjected to *in vivo* endothelial **(*B*, n=4)** or vascular **(*C*, n=6)** permeability assay using microspheres or Evans blue. Arrowheads indicate the inter-endothelial gaps between VE-cadherin junctions **(*A*)** and the leakage site for G-spheres **(*B*)**. Whole segments of mouse aortas were subjected to Evans blue staining to examine dye leakage in these mice **(*C*)**. Quantitative data of the results in ***A*** and ***B*** are shown in *Figures 6A* and *6B*, respectively. Data are means±SEM and were analyzed by a two-tailed Student *t*-test (n=6 per group). **(*D*-*F*)** Representative photomicrographs of picrosirius red staining **(*D*)**, Movat pentachrome staining **(*E*)**, and co-immunohistochemical staining for αSMA (green), vimentin (Vim) (red), and IB4 (white) **(*F*)** in the lesions of *ApoE*$^{-/-}$ mice. NC, necrotic core. All studies were performed on the sections of the innominate artery and the IA region of mice, and quantitative data are shown in *Figures 6E-6H*. Results represent at least three independent experiments with similar results.

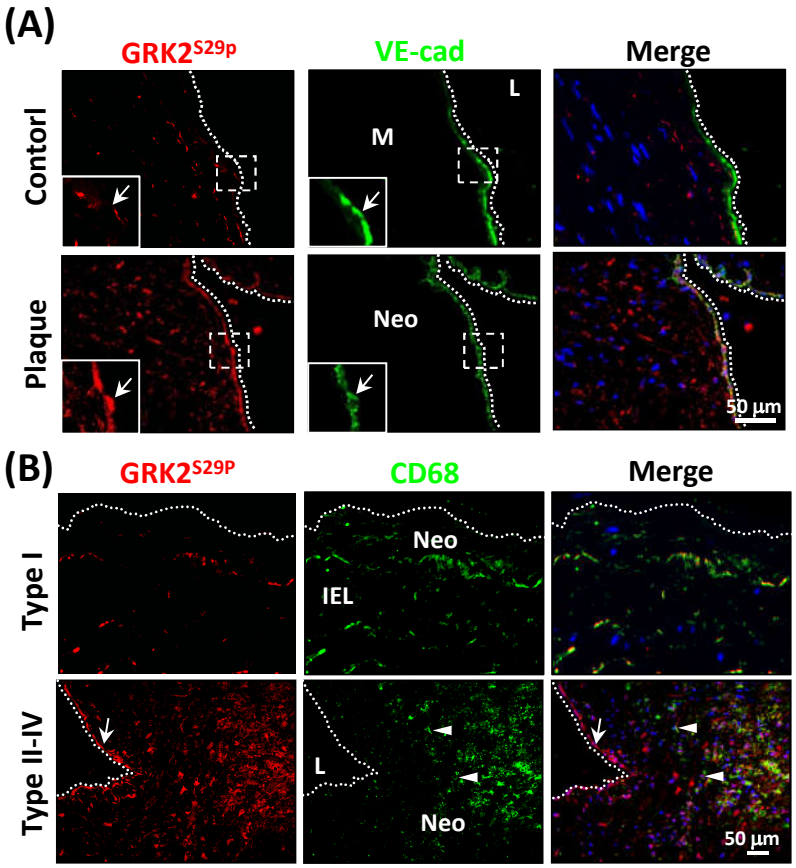

Supplementary Figure S12. The expression levels of GRK2^{S29p} in the endothelial layer of human atheromas. **(*A*)** Cross-sections of diseased human coronary arteries and control internal thoracic arteries were co-immunostained for GRK2^{S29p} (red) and VE-cadherin (green). Left-lower panels in each picture show the magnified views of the indicated areas (white dashed line box). **(*B*)** Cross-sections of different types of atheromas were co-immunostained for GRK2^{S29p} (red) and macrophage marker CD68 (green). Cell nuclei were counterstained with DAPI. Arrow indicates GRK2^{S29p}-positive EC layers. Arrowheads indicate CD68-positive macrophages. The white dotted lines indicate the margin of the vessel lumen. IEL, internal elastic lamina. L, lumen. M, medial region. Neo, neointima. The pictured images represent at least six independent experiments with similar results.

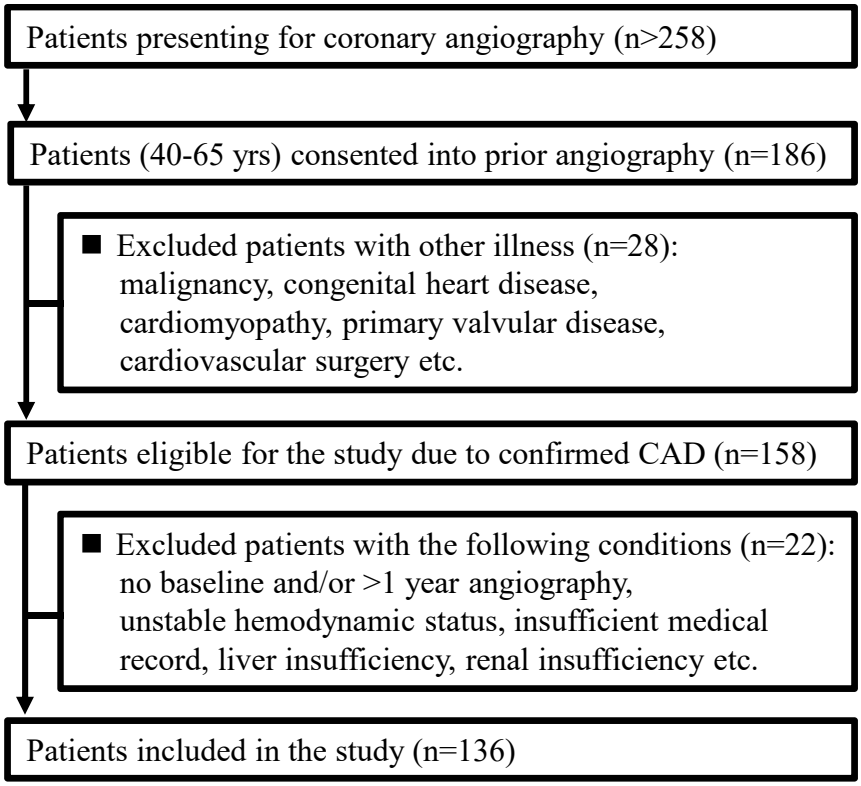

Supplementary Figure S13. Study flowchart for collecting sera from patients with CAD.

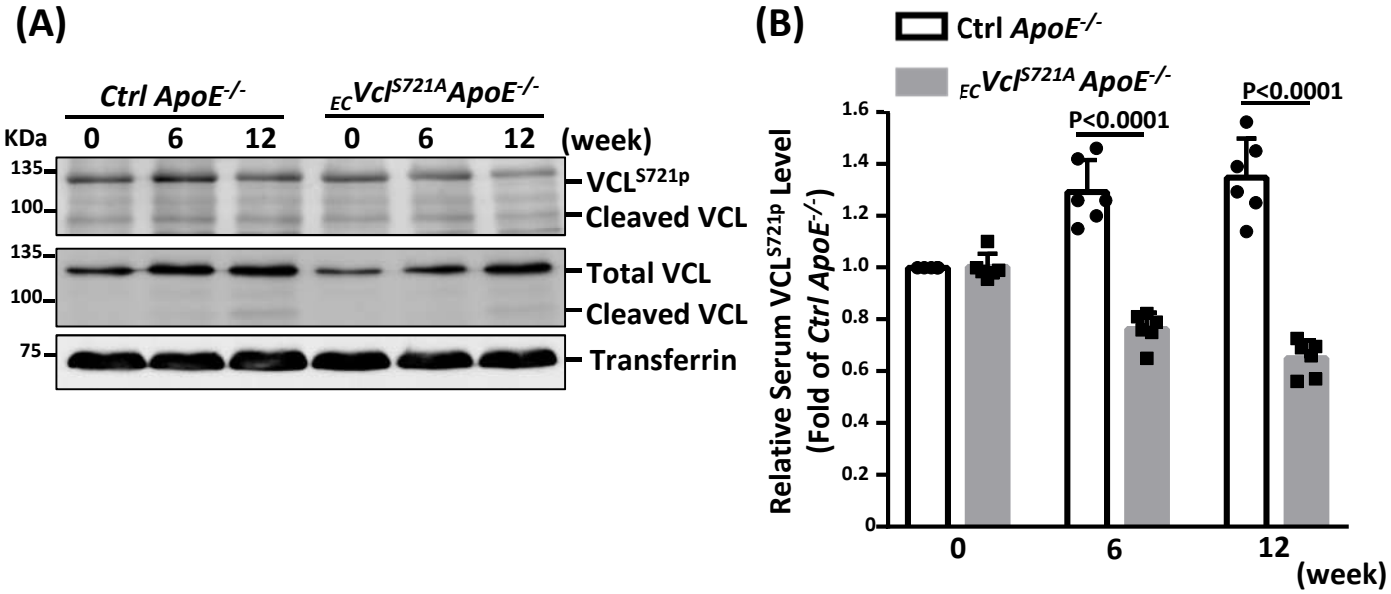

Supplementary Figure S14. The serum level of VCP^{S721p} in $_{EC}Vcl^{S721A}ApoE^{-/-}$ mice is reduced during the progression of atherosclerosis. (*A*) Total sVCL and sVCL^{S721p} levels in the sera of $_{EC}Vcl^{S721A}ApoE^{-/-}$ and control *ApoE*$^{-/-}$ mice fed an HCD for the indicated times. Western blot analysis of the full-length VCL (~124 kDa) and its cleaved form (~95 kDa) in mouse sera. Results represent duplicate experiments with similar results. **(*B*)** Quantitative analysis of the relative sVCL^{S721p} levels in $_{EC}Vcl^{S721A}ApoE^{-/-}$ and control *ApoE*$^{-/-}$ mice fed an HCD for the indicated times. n=6 per group. Data were analyzed by two-way ANOVA with Tukey multiple comparison test and are presented as means±SEM (n=6).

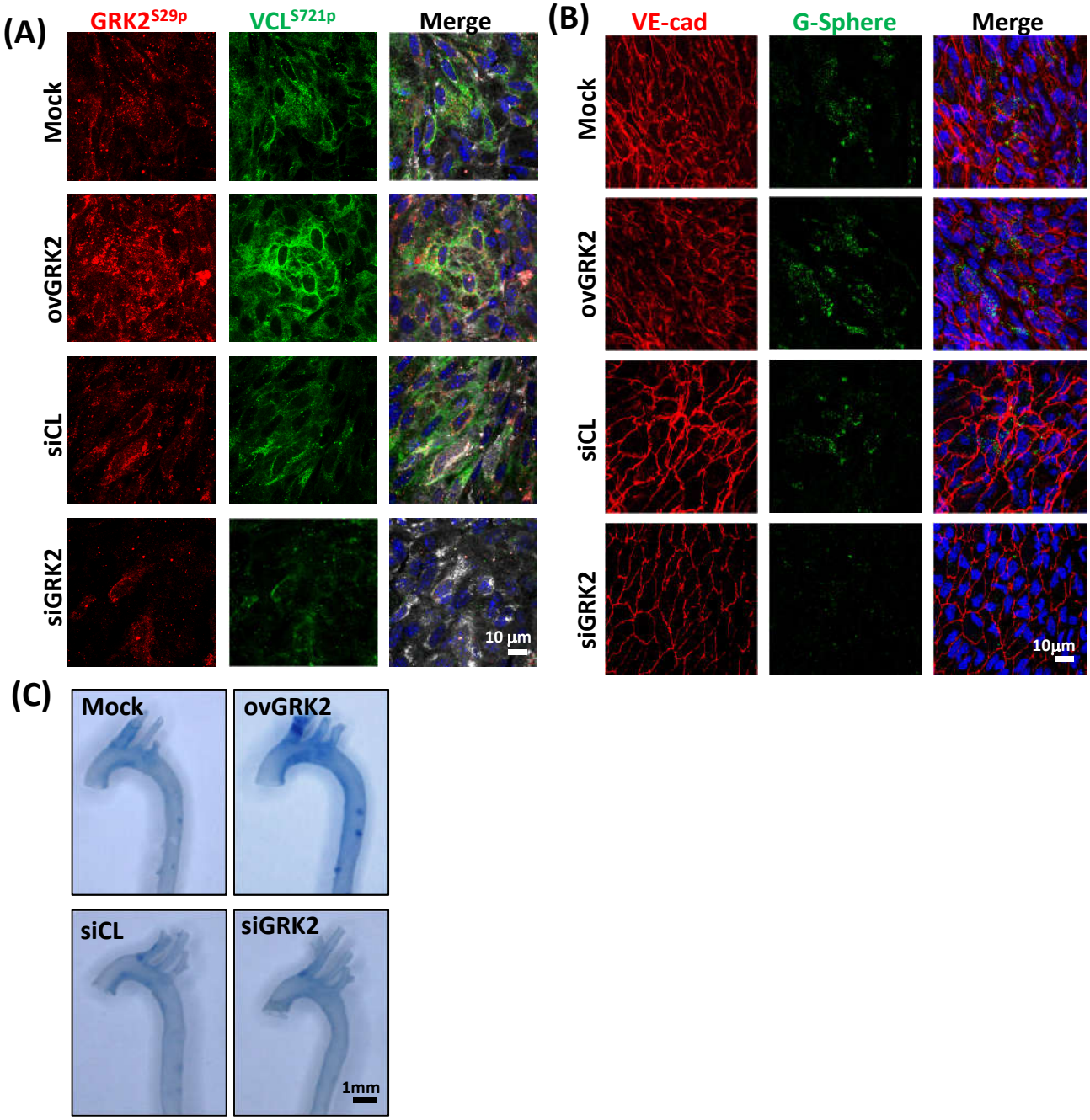

Supplementary Figure S15. GRK2 is pivotal to VCL phosphorylation in ECs. *ApoE*$^{-/-}$ mice (6 weeks old, 20~25 g) were administrated with GRK2-overexpressing plasmid (ovGRK2, 2 μg DNA/g, every 3 d) or GRK2-specific siRNA (siGRK2, 0.1 μg siRNA/g, every 3 d) *via* intravenous injection with *in vivo* Turbofect Reagent and *invivofectamine*® for six weeks. Mice that received mock plasmid or control siRNA (siCL) were used as controls. **(*A*)** *En-face* fluorescence photomicrographs of the endothelium in the IA co-immunostained for GRK2^{S29p} (red) and VCL^{S721p} (green), with endothelial IB4 staining (white) and DAPI nuclear counterstains (blue). **(*B* and *C*)** Whole segments of aortas were subjected to *in vivo* endothelial and vascular permeability assays using FITC-conjugated microspheres **(*B*)** and Evans blue dye **(*C*)**, respectively. **(*B*)** Representative images of *en-face* immunostaining for VE-cadherin (red) and fluorescent polymer microspheres (G-spheres, 0.1 μm in size, green) in the endothelium of the IA region. Cell nuclei were counterstained with DAPI. The pictured images represent duplicate experiments with similar results.

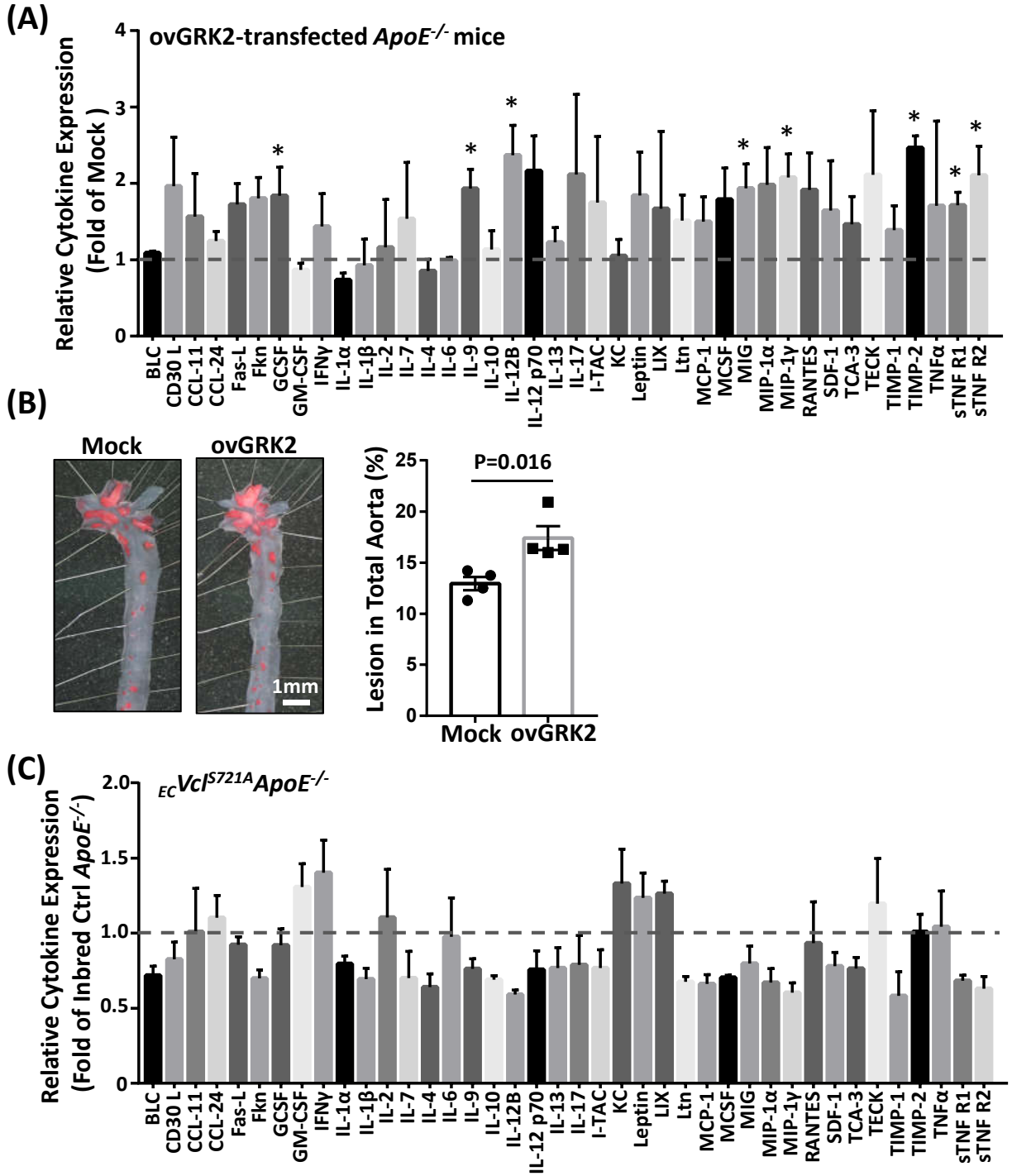

Supplementary Figure S16. Overexpression of GRK2 increases the serum levels of cytokines and atherosclerotic lesions in *ApoE*$^{-/-}$ mice. (*A* and *B*) *ApoE*$^{-/-}$ mice (6 weeks old) were administrated with GRK2-overexpressing plasmid (ovGRK2) or mock control (2 μg DNA/g, every 3 d) *via* intravenous injection by *in vivo* Turbofect Reagent for 6 **(*A*)** or 12 weeks **(*B*)** (n=3~4 each). **(*A* and *C*)** Mouse sera were collected, and the systemic levels of circulating inflammatory cytokines were determined using a mouse inflammatory cytokine array, as described in the Supplemental Methods. **(*A*)** Signal detection by ECL showed that the expression levels of cytokines, including IL-9, IL-12B, MIP-1γ, sTNF R1, and sTNF R2, in the serum of ovGRK2-administrated *ApoE*$^{-/-}$ mice were significantly higher than those in mock control *ApoE*$^{-/-}$ mice (n=3). * $p<0.05$ *vs*. control mice **(*B*)** Whole aortas were dissected and stained with Oil-red O to quantify lesion areas (n=4 per group). **(*C*)** Detection of systemic levels of circulating cytokines in the serum of $_{EC}Vcl^{S721A}ApoE^{-/-}$ *vs*. inbred control *ApoE*$^{-/-}$ mice fed an HCD for 6 weeks. Signal detection by ECL showed no significant difference in the expression profiles of indicated circulating cytokines between $_{EC}Vcl^{S721A}ApoE^{-/-}$ and control *ApoE*$^{-/-}$ mice. The manufacturer provides detailed information on each cytokine's instructions, including abbreviation and function (133999, Abcam). Data are presented as means ± SEM from three independent experiments and were analyzed by a two-tailed Student *t*-test.

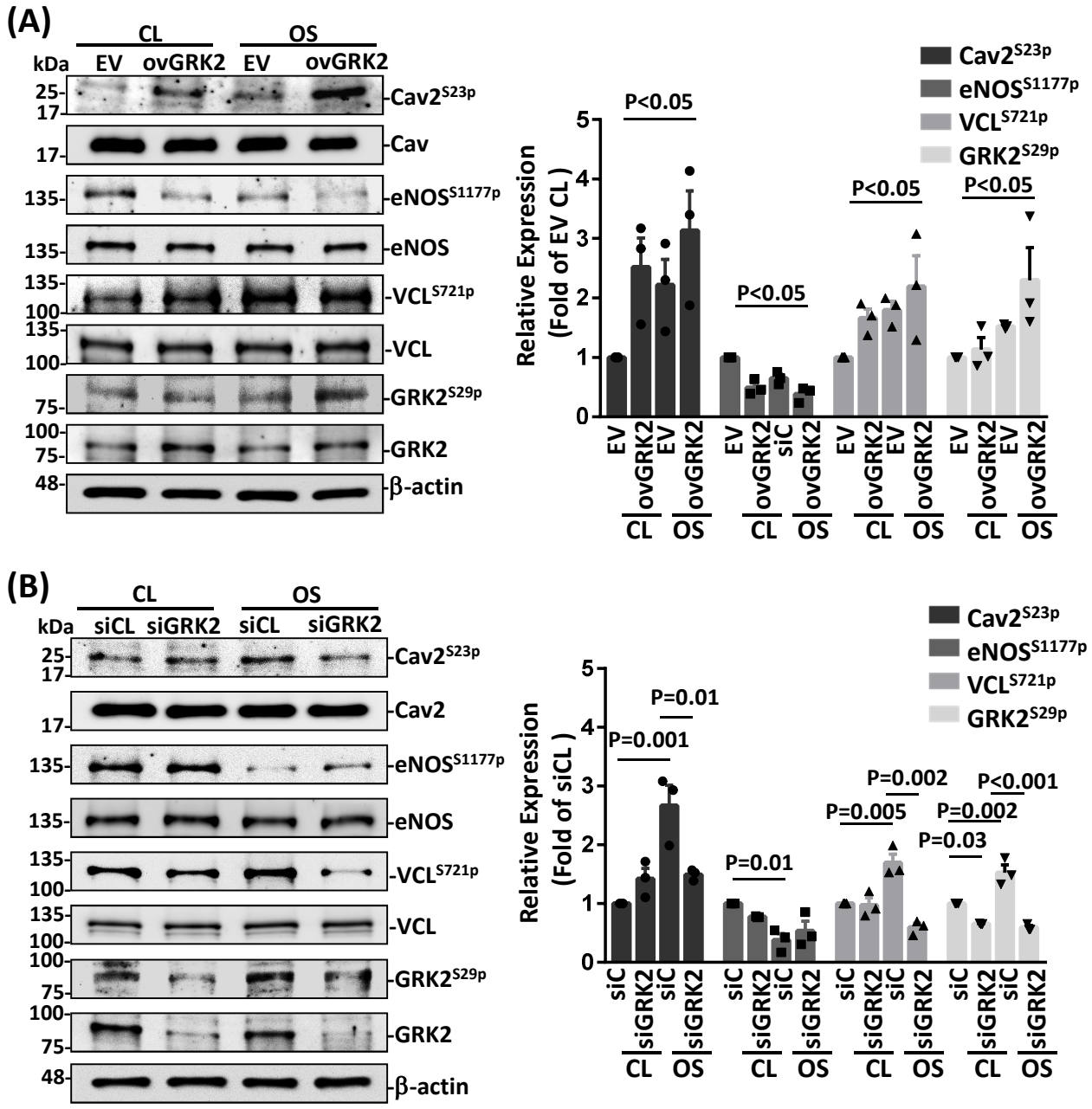

Supplementary Figure S17. GRK2 can modulate Cav2 and eNOS phosphorylations in ECs in response to disturbed flow. ECs were transfected with GRK2-overexpressing plasmid (ovGRK2; 1.0 μg DNA/mL) or GRK2-specific siRNA (siGRK; 15 nM each) for 24 h and then kept in static condition (CL) or exposed to oscillatory shear stress (OS) for 24 h. Empty vector (EV) and scramble siRNA control (siCL) were used as control groups. Representative data of Western blot analysis of the Cav2, Cav2^{S23p}, eNOS, eNOS^{S1177p}, VCL^{S721p}, VCL, GRK^{S29p}, and GRK2 expressions in GRK2-overexpressed **(*A*)** or siGRK2-transfected ECs **(*B*)**. Data are means ± SEM from three independent experiments and were analyzed by two-way ANOVA with Tukey multiple comparison test.

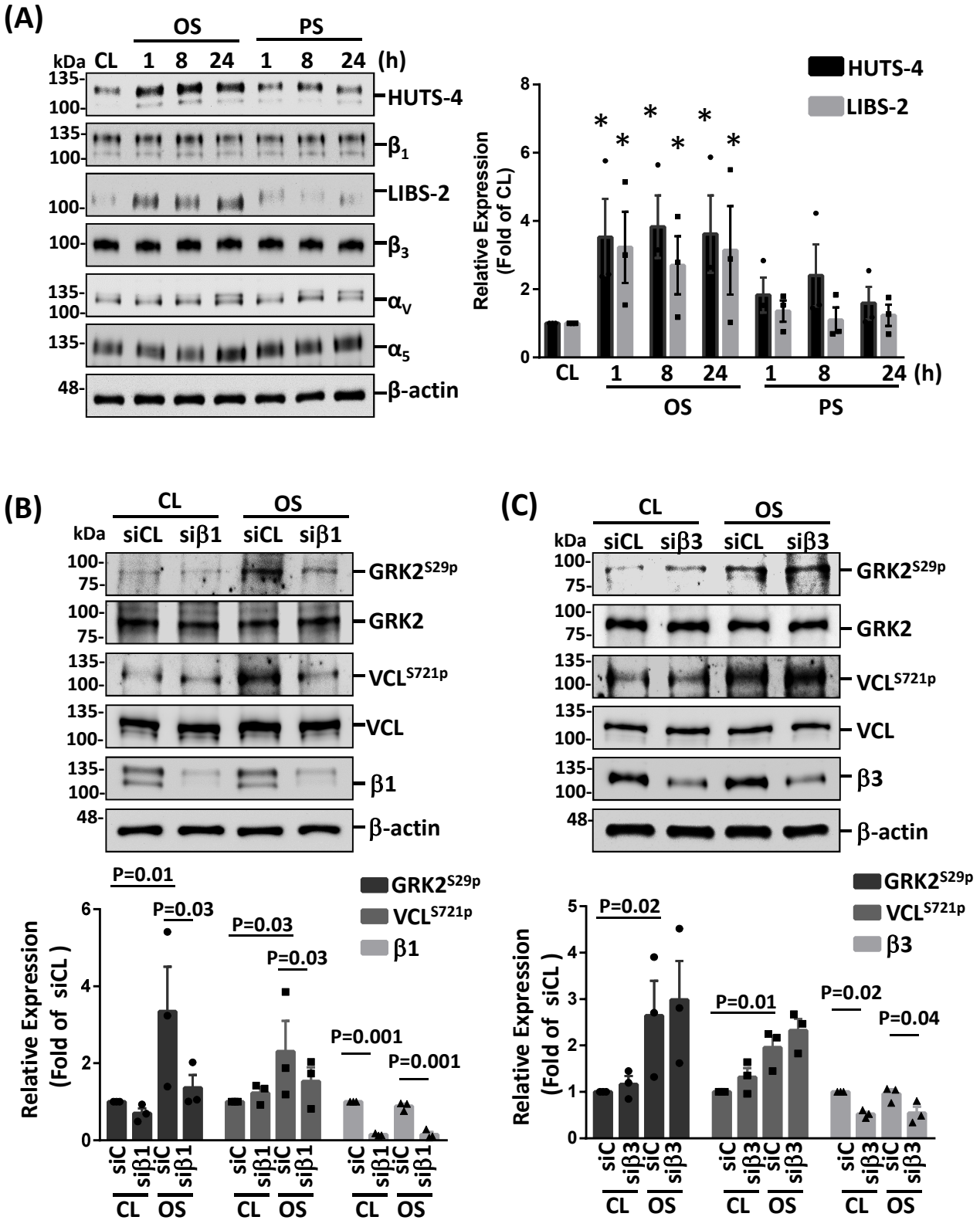

Supplementary Figure S18. β_1 integrin is involved in OS-inductions of GRK2^{S29p} and VCL^{S721p} in ECs. ECs were kept in static condition (CL) or exposed to oscillatory (OS) or pulsatile (PS) shear stress for the indicated time **(*A*)** or 24 h (***B*** and ***C***). (***A***) The expressions of HUTS-4 (active β_1), β_1, LIBS-2 (active β_3), β_3, α_V, and α_5 integrins were examined by Western blot analysis. β_1- (siβ_1) **(*B*)** and β_3-specific (siβ_3) siRNAs **(*C*)** (50 nM each) were transfected into ECs before the flow experiments. Scramble siRNA (siCL) was used as a control. Data are means ± SEM from three independent experiments and were analyzed by one-way ANOVA with Dunnett's multiple comparison test **(*A*)** or two-way ANOVA with Tukey multiple comparison test **(*B* and *C*).**

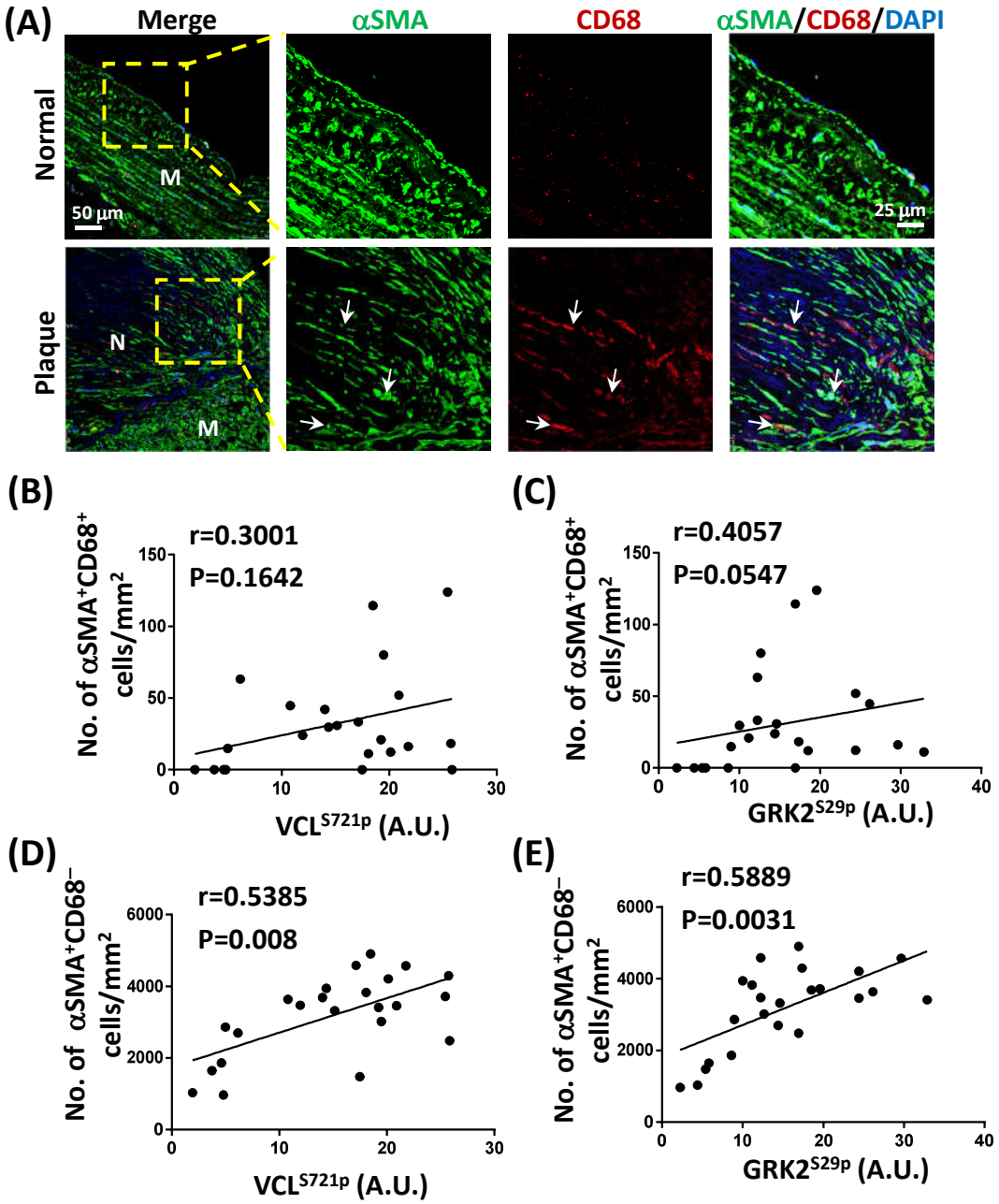

Supplementary Figure S19. The numbers of αSMA^{+}CD68^{+} cells in human atherosclerotic lesions do not show correlations with the levels of EC VCL^{S721p} and GRK2^{S29p}. (***A***) Representative images showing the co-immunohistochemical staining of the cross-sections of diseased human coronary arteries for SMC marker αSMA (green) and macrophage marker CD68 (red) for identifying macrophage-like SMCs (i.e., αSMA^{+}CD68^{+} cells, arrows). Cell nuclei were counterstained with DAPI. The right panels are the magnified views of the indicated areas (yellow dashed line box) in the left panels. M, medial layers. N, Neointima. (***B-E***) The scatter plots of the associations between the average fluorescence intensities (arbitrary units, A.U.) of endothelial VCL^{S721p} (***B*** and ***D***) and GRK2^{S29p} (***C*** and ***E***) and the numbers of αSMA^{+}CD68^{+} cells (***B*** and ***C***) and αSMA^{+}CD68^{-} cells (***D*** and ***E***) in the examined human atheroma sections (n=23). *P* values and correlation coefficients (r) were calculated by using Spearman's rho correlation test.

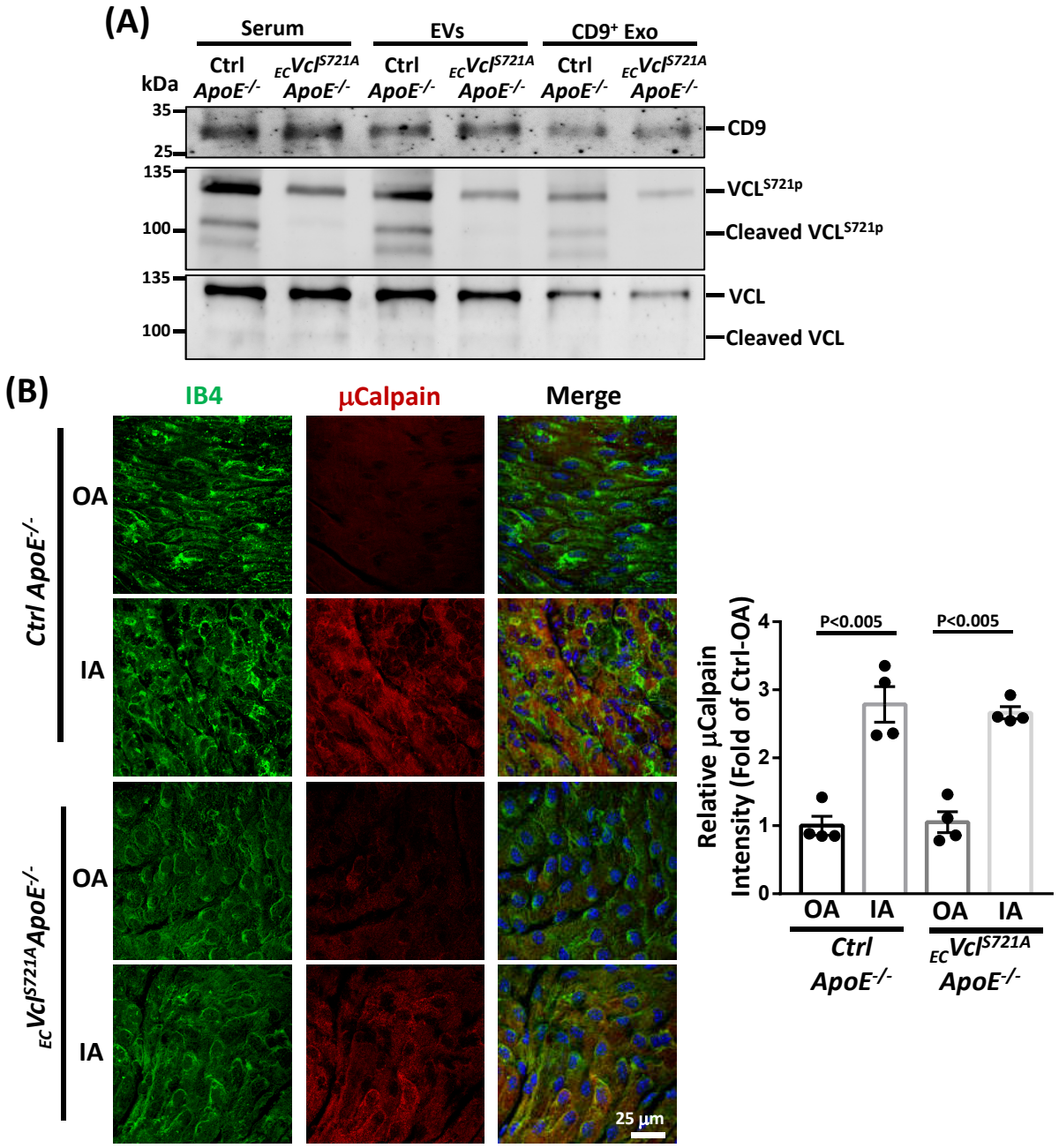

Supplementary Figure S20. The distribution profiles of sVCL^{S721p} and sVCL and the calpain expression in vascular endothelium in $_{EC}Vcl^{S721A}ApoE^{-/-}$ mice. Six-week-old $_{EC}Vcl^{S721A}ApoE^{-/-}$ mice and inbred control *ApoE*$^{-/-}$ mice were fed an HCD for 12 weeks (n=4 each). Mouse serum was collected, and the distributions of extracellular vesicles (EVs)/exosomes (Exo)-shuttled sVCL^{S721p} and total sVCL in the serum were examined by Western blot analysis. Tetraspanins CD9 was used as an exosome biomarker and for normalization in Western blot analysis. **(*A*)** Western blot analysis of full-length and cleaved forms of sVCL^{S721p} and total sVCL in the serum, EVs, and exosomes. Results represent duplicate experiments with similar results. **(*B*)** Segments of aortic arch were collected and subjected to *en-face* immunostaining for examining the µ-calpain (i.e., the active form of calpain) expression in vascular endothelium in different flow areas. Isolectin B4 (IB4), used as an EC marker, was co-immunostained. Cell nuclei were counterstained with DAPI. IA, inner curvature of the aortic arch. OA, outer curvature of the aortic arch. Data were analyzed by a two-tailed Student *t*-test and are presented as means ± SEM (n=4). The pictured images represent four independent experiments with similar results.

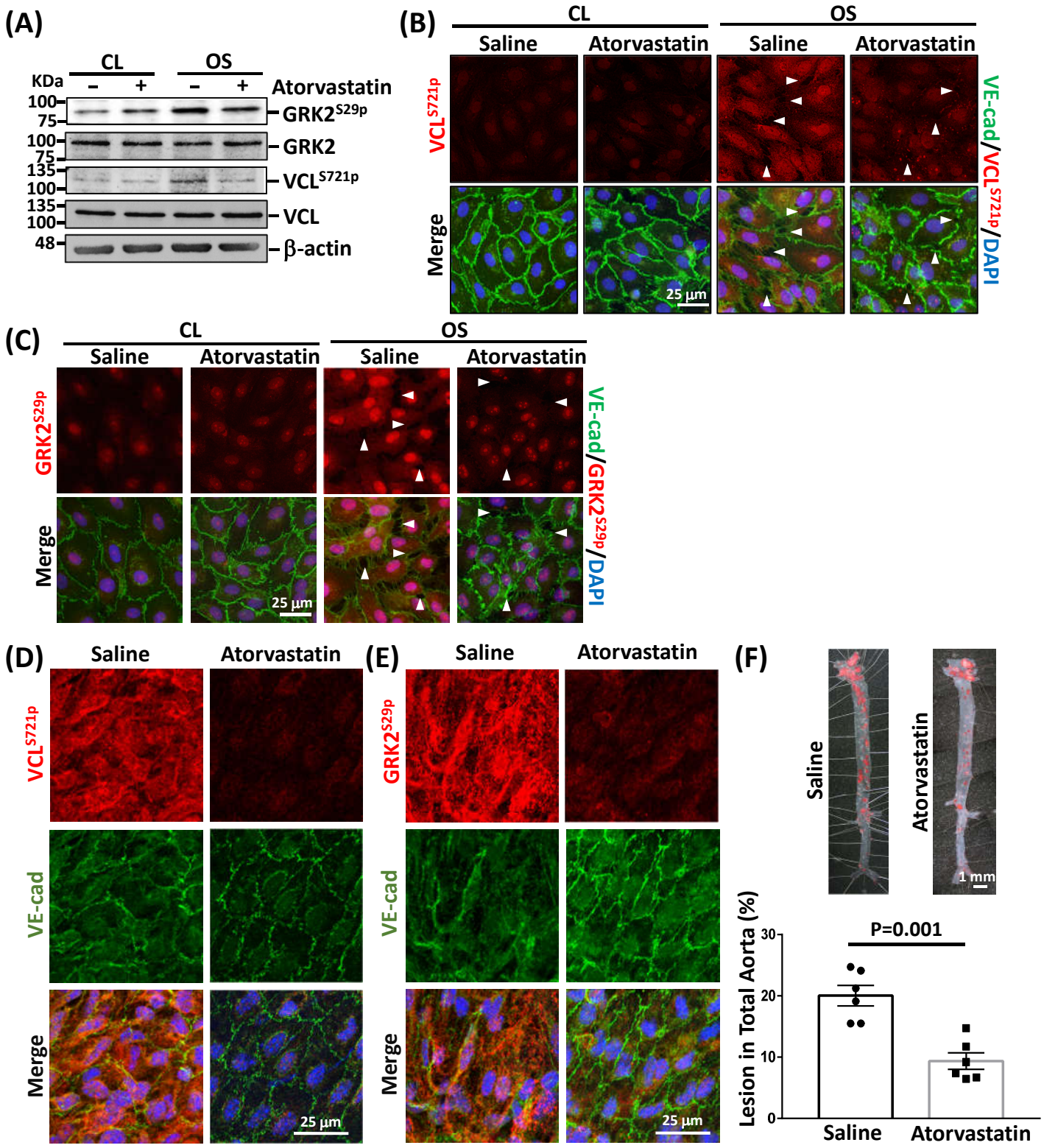

Supplementary Figure S21. Atorvastatin treatment inhibits OS-induction of GRK^{S29p} and VCL^{S721p} in ECs and reduces plaque formation in *ApoE*$^{-/-}$ mice. (***A-C***) ECs were pre-treated with atorvastatin (1 μM) and subjected to oscillatory shear stress (OS) for 24 h, and the levels of GRK2, VCL, and their phosphorylated molecules were examined by Western blot analysis (***A***) and immunocytochemical staining (***B*** and ***C***). Arrowheads indicate the gap areas of the VE-cadherin junction. (***D-F***) *ApoE*$^{-/-}$ mice were fed an HCD and treated with atorvastatin (10 mg/kg/d) by oral administration for 6 weeks (***D*** and ***E***) and 12 weeks (***F***). *En-face* immunostaining was performed to detect the expression levels of VCL^{S721p} (***D***, red), GRK2^{S29p} (***E***, red), and endothelial VE-cadherin (***D*** and ***E***, green) in the vascular endothelium of IA in *ApoE*$^{-/-}$ mice. Cell nuclei were counterstained with DAPI. (***F***) Whole aortas were dissected from saline- or atorvastatin-treated *ApoE*$^{-/-}$ mice and stained with Oil-red O to quantify lesion areas (n=6 per group). Data in ***F*** are means±SEM and were analyzed by a two-tailed Student *t*-test. Images shown in each picture in ***A*** to ***E*** represent duplicate experiments with similar results.